

NASA/CR-2007-214885/VOL2



Hypervelocity Impact (HVI)

*Volume 2: WLE Small-Scale Fiberglass Panel Flat
Multi-Layer Targets A-1, A-2, and B-1*

*Michael R. Gorman and Steven M. Ziola
Digital Wave Corporation, Englewood, Colorado*

September 2007

The NASA STI Program Office . . . in Profile

Since its founding, NASA has been dedicated to the advancement of aeronautics and space science. The NASA Scientific and Technical Information (STI) Program Office plays a key part in helping NASA maintain this important role.

The NASA STI Program Office is operated by Langley Research Center, the lead center for NASA's scientific and technical information. The NASA STI Program Office provides access to the NASA STI Database, the largest collection of aeronautical and space science STI in the world. The Program Office is also NASA's institutional mechanism for disseminating the results of its research and development activities. These results are published by NASA in the NASA STI Report Series, which includes the following report types:

- **TECHNICAL PUBLICATION.** Reports of completed research or a major significant phase of research that present the results of NASA programs and include extensive data or theoretical analysis. Includes compilations of significant scientific and technical data and information deemed to be of continuing reference value. NASA counterpart of peer-reviewed formal professional papers, but having less stringent limitations on manuscript length and extent of graphic presentations.
- **TECHNICAL MEMORANDUM.** Scientific and technical findings that are preliminary or of specialized interest, e.g., quick release reports, working papers, and bibliographies that contain minimal annotation. Does not contain extensive analysis.
- **CONTRACTOR REPORT.** Scientific and technical findings by NASA-sponsored contractors and grantees.

- **CONFERENCE PUBLICATION.** Collected papers from scientific and technical conferences, symposia, seminars, or other meetings sponsored or co-sponsored by NASA.
- **SPECIAL PUBLICATION.** Scientific, technical, or historical information from NASA programs, projects, and missions, often concerned with subjects having substantial public interest.
- **TECHNICAL TRANSLATION.** English-language translations of foreign scientific and technical material pertinent to NASA's mission.

Specialized services that complement the STI Program Office's diverse offerings include creating custom thesauri, building customized databases, organizing and publishing research results ... even providing videos.

For more information about the NASA STI Program Office, see the following:

- Access the NASA STI Program Home Page at <http://www.sti.nasa.gov>
- E-mail your question via the Internet to help@sti.nasa.gov
- Fax your question to the NASA STI Help Desk at (301) 621-0134
- Phone the NASA STI Help Desk at (301) 621-0390
- Write to:
NASA STI Help Desk
NASA Center for AeroSpace Information
7115 Standard Drive
Hanover, MD 21076-1320

NASA/CR-2007-214885/VOL2



Hypervelocity Impact (HVI)

Volume 2: WLE Small-Scale Fiberglass Panel Flat Multi-Layer Targets A-1, A-2, and B-1

*Michael R. Gorman and Steven M. Ziola
Digital Wave Corporation, Englewood, Colorado*

National Aeronautics and
Space Administration

Langley Research Center
Hampton, Virginia 23681-2199

Prepared for Langley Research Center
under Contract NNL05AC19T

September 2007

The use of trademarks or names of manufacturers in this report is for accurate reporting and does not constitute an official endorsement, either expressed or implied, of such products or manufacturers by the National Aeronautics and Space Administration.

Available from:

NASA Center for AeroSpace Information (CASI)
7115 Standard Drive
Hanover, MD 21076-1320
(301) 621-0390

National Technical Information Service (NTIS)
5285 Port Royal Road
Springfield, VA 22161-2171
(703) 605-6000



Hypervelocity Impact (HVI)

WLE Small-Scale Fiberglass Panel Flat Multi-Layer Targets A-1, A-2 and B-1

During 2003 and 2004, the Johnson Space Center's White Sands Testing Facility in Las Cruces, New Mexico conducted hypervelocity impact tests on the space shuttle wing leading edge.

Hypervelocity impact tests were conducted to determine if Micro-Meteoroid/Orbital Debris impacts could be reliably detected and located using simple passive ultrasonic methods.

The objective of Targets A-1, A-2, and B-2 was to study hypervelocity impacts through multi-layered panels simulating Whipple shields on spacecraft.

Impact damage was detected using lightweight, low power instrumentation capable of being used in flight.

Table of Contents

Introduction.....	5
Experimental Description.....	6
Results.....	18
Discussion.....	20
Target A-1.....	21
Target A-2.....	23
Target B-1.....	24
Location Analysis.....	27
Wave Propagation.....	27
Conclusions.....	28
Appendix.....	29
Test Conditions Data Sheets.....	33
Data Tables.....	62

List of Figures

Figure 1: Target A-1. Left: Top View. Right: Bottom View.....	7
Figure 2: Target A-1 Drawing.....	7
Figure 3: Target A-2 Left: Top View. Right: Bottom View.....	8
Figure 4: Target A-2 Drawing.....	8
Figure 5: Target B-1. Left: Top View. Right: Bottom View.....	9
Figure 6: Target B-1 Drawing.....	9
Figure 7: Fiberglass Panel Target with 90 deg Impact Angle. Back Side View.....	10
Figure 8: Detail of Sensors on Targets A-1 (left) and A-2 (right).....	10
Figure 9: Diagram of Sensor Locations on Fiberglass Panel Target A-1. Front View....	11
Figure 10: Diagram of Sensor Locations on Aluminum Back Plate Target A-1. Front View.....	11
Figure 11: Diagram of Sensor Locations on Fiberglass Panel Target A-2. Front View..	12
Figure 12: Diagram of Sensor Locations on Aluminum Back Plate Target A-2. Front View.....	12
Figure 13: Diagram of Sensor Locations on Fiberglass Plate 1 Target B-1. Front View.	13
Figure 14: Diagram of Sensor Locations on Fiberglass Plate 2 Target B-1. Front View.	13
Figure 15: Diagram of Sensor Locations on Aluminum Back Plate Target B-1. Front View.....	14
Figure 16: Example of DC Offset.....	15
Figure 17: A-2 Impact Signal for Shot #11.....	16
Figure 18: Detail of A-2 Impact Signal for Shot #11, Sensors 2 and 4.....	16
Figure 19: A-2 Electromagnetic Interference for Shot #11.....	17
Figure 20: A-1 Shot #5 Impact Damage.....	19
Figure 21: B-1 Shot #10 Impact Damage.....	19
Figure 22: A-2 Shot #13 Impact Damage.....	20
Figure 23: Multilayer Penetration Mechanisms.....	21

Figure 24: Impact Waveform for Shot #1. Notice the missing signal for sensor 5 in the bottom left corner..... 22

Figure 25: Shot #5 Impact Waveform. Notice saturation on channels 1-4. Channels 2 and 6 have shortened signals due to sensors being knocked off during impact. 22

Figure 26: Wave Signal Energy vs. Kinetic Energy on A-2 Fiberglass Plate (Sensors 5 and 6)..... 23

Figure 27: Wave Signal Energy vs. Kinetic Energy for A-2 Aluminum Back Plate (Sensors 1-4)..... 24

Figure 28: Shot #3 Impact Waveform, Sensor 6 (left) and Shot #7 Impact Waveform, Sensor 6 (right) 25

Figure 29: Shot #9 Impact Waveform..... 25

Figure 30: Shot #10 Impact Waveform..... 26

Figure 31: Shot #7 Impact Waveform, Sensors 1-8..... 27

Figure 32: Target A-1 Drawing 30

Figure 33: Target B-1 Drawing 31

Figure 34: Target A-2 Drawing 32

Figure 35: A-1 Shot #1 Impact Waveform..... 34

Figure 36: A-1 Shot #1 Impact Damage 34

Figure 37: A-1 Shot #2 Impact Waveform..... 36

Figure 38: A-1 Shot #2 Impact Damage 36

Figure 39: A-1 Shot #3 Impact Waveform..... 38

Figure 40: A-1 Shot #3 Impact Damage 38

Figure 41: A-1 Shot #5 Impact Waveform..... 40

Figure 42: A-1 Shot #5 Impact Damage 40

Figure 43: A-1 Shot #6 Impact Waveform..... 42

Figure 44: A-1 Shot #6 Impact Damage 42

Figure 45: B-1 Shot #7 Impact Waveform..... 44

Figure 46: B-1 Shot #7 Impact Waveform..... 44

Figure 47: B-1 Shot #8 Impact Waveform..... 46

Figure 48: B-1 Shot #8 Impact Damage..... 46

Figure 49: B-1 Shot # 9 Impact Waveform..... 48

Figure 50: B-1 Shot # 9 Impact Damage..... 48

Figure 51: B-1 Shot #10 Impact Waveform 50

Figure 52: B-1 Shot #10 Impact Damage..... 50

Figure 53: A-2 Shot #11 Impact Waveform..... 52

Figure 54: A-2 Shot #11 Impact Damage..... 52

Figure 55: A-2 Shot #12 Impact Waveform..... 54

Figure 56: A-2 Shot #12 Impact Damage..... 54

Figure 57: A-2 Shot #13 Impact Waveform..... 56

Figure 58: A-2 Shot #13 Impact Damage..... 56

Figure 59: A-2 Shot #14 Impact Waveform..... 58

Figure 60: A-2 Shot #14 Impact Damage..... 58

Figure 61: A-2 Shot #15 Impact Waveform..... 60

Figure 62: A-2 Shot #15 Impact Damage..... 60

List of Tables

Table 1: Kinetic Energy and Wave Signal Energy for Fiberglass Panel Target A-1, B-1, and A-2	18
Table 2: Damage Results for Fiberglass Panel Targets A-1, B-1 and A-2.....	19
Table 3: A-1, B-1, and A-2 Impactor Diameter, Impactor Velocity, Impactor Angle, Kinetic Energy, and Location	62
Table 4: A-1, B-1, and A-2 Damage Results.....	62
Table 5: A-1, B-1, and A-2 Raw Wave Signal, Sensors 1-8	63
Table 6: A-1, B-1, and A-2 Channel Gain Settings	64
Table 7: A-1, B-1, and A-2 Wave Signal Energy, Sensors 1-8 and Total Wave Signal Energy	64

Hypervelocity Impact (HVI)

Volume 2: WLE Small-Scale Fiberglass Panel Flat Targets A-1, A-2, and B-1

Introduction

In the wake of the Columbia accident, NASA personnel decided to test the idea that impacts during space flight could be detected by acoustical sensors at ultrasonic frequencies. The substance of this idea rested on the knowledge that in laboratory experiments lower velocity impacts had created signals with frequencies in the 20 – 200 kHz range. If Shuttle engine and aerodynamic noise were down in the sonic range then locating impacts would be easier in the 20-200 kHz range. The questions were what frequencies would be created during hypervelocity impacts by tiny objects, what would their energies be, and what would be the best way to detect them, keeping in mind the potential need for lightweight, simple installation procedures and low electrical energy consumption.

A further basis for selecting this method was that recent fundamental research had elucidated the basic physics of the ultrasonic signals created by the impacts in a variety of aerospace materials and geometries. This made it more likely that signal and noise could be separated and that subsequent analysis of the signals would yield the desired information about impact severity and location. All of the above reasoning proved to be correct. Hypervelocity impact by tiny aluminum spheres created signals in the 20-200 kHz frequency range easily detectable with small piezoelectric sensors similar to equipment being flown.

Targets A-1, A-2, and B-1 were three of several targets (see below) used for hypervelocity impact testing. There is a section in this Report for each of the other targets. The structure of this report includes a General Introduction that contains the overall goals, the personnel involved, the test methods, instrumentation, calibration, and overall results and conclusions. Only abbreviated descriptions of the test methods, instrumentation, and calibration are given in each of the Target sections such as this one.

This section describes Targets A-1, A-2, and B-1, the test equipment, features tables of kinetic energy and damage results, and discusses the linear relationship between kinetic energy, ultrasonic wave signal energy and damage. Also discussed are wave propagation effects, the wave modes and their velocities, and location of impacts by analysis of wave arrival times.

The Appendix has test condition data sheets, impact waveforms, and photos of the damage for each shot. Also included are tables of impact data, gain settings, recorded wave signals, and damage results.

The number of targets tested in the overall HVI study was extensive as shown in the list below:

- A-1 – Fiberglass plate and aluminum plate with standoff rods (with grommets)
- A-2 – Fiberglass plate and aluminum plate with standoff rods (no grommets)
- B-1 – Two fiberglass plates and aluminum plate with standoff rods
- C-1 – Fiberglass flat plate
- C-2 – Fiberglass flat plate
- Fg(RCC)-1 – Fiberglass in the shape of Wing Leading Edge
- Fg(RCC)-2 – Fiberglass in the shape of Wing Leading Edge
- RCC16R – Carbon-Carbon Actual WLE
- A-1 Tile – Tile structure of forward part of wing with no gap filler
- Ag-1 Tile – Tile structure of forward part of wing with gap filler
- B-1 Tile – Tile structure of aft part of wing with no gap filler
- Bg-1 Tile – Tile structure of aft part of wing with gap filler

It is everyday experience that when a solid material is struck, sound is created. This new passive ultrasonic technique has been designated modal acoustic emission (MAE) due to its (physical) similarity to an older, but less robust technique known as acoustic emission. In structures built of plate-like sections (aircraft wings, fuselages, etc.) the sound waves of interest are the extensional mode (in-plane stretching and compressing of the plate) and the flexural mode (bending of the plate). These are called plate waves and they propagate in bounded media where the wavelength of the wave is larger than the thickness of the plate. The frequency spectrum typically ranges from the low kilohertz to about one megahertz. Plate waves can be detected with simple piezoelectric transducers that convert mechanical motion into electrical voltage.

By analyzing mode shapes, and taking into account the material and loading, sources can be identified and located. The direct connection to fundamental physics is a key characteristic of MAE. For simple geometries the wave shapes and velocities have been calculated from wave equations derived from Newton's laws of motion and they compare well with measurements. (See General Introduction to this report for a fuller discussion of modal AE.) By using arrival times at transducers with known positions, the location of the source can be triangulated by various mathematical methods (similar to methods used in SONAR).

Experimental Description

Targets A-1 and A-2 consisted of a fiberglass front plate followed by an aluminum backplate. Target size was 30" x 30", with 0.25" thick fiberglass and 1/8" thick aluminum. Standoff between the fiberglass and aluminum was 12". The plates were connected using (8) 0.5" all-thread rods. L-shaped angles added to the back of the aluminum plate were used to attach the target to a target support stand, which was placed in the target chamber. The fiberglass panel was a 19 ply (0.90) woven material. Target A-1 contained grommets that isolated the fiberglass panel from the all-thread (see Figure 1 and Figure 2).

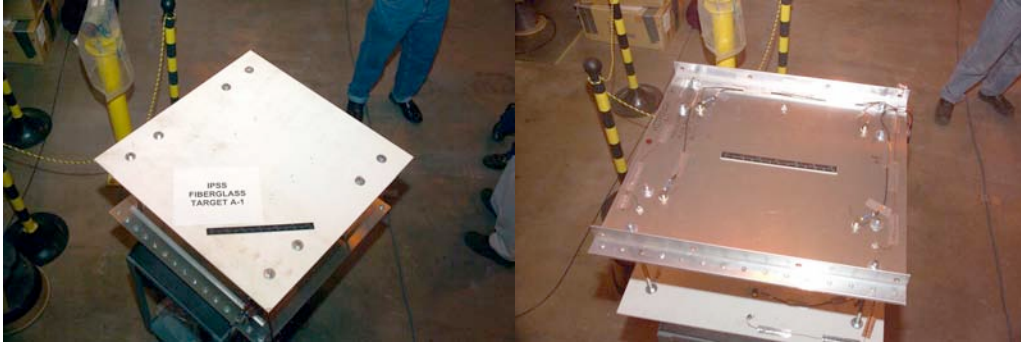


Figure 1: Target A-1. Left: Top View. Right: Bottom View.

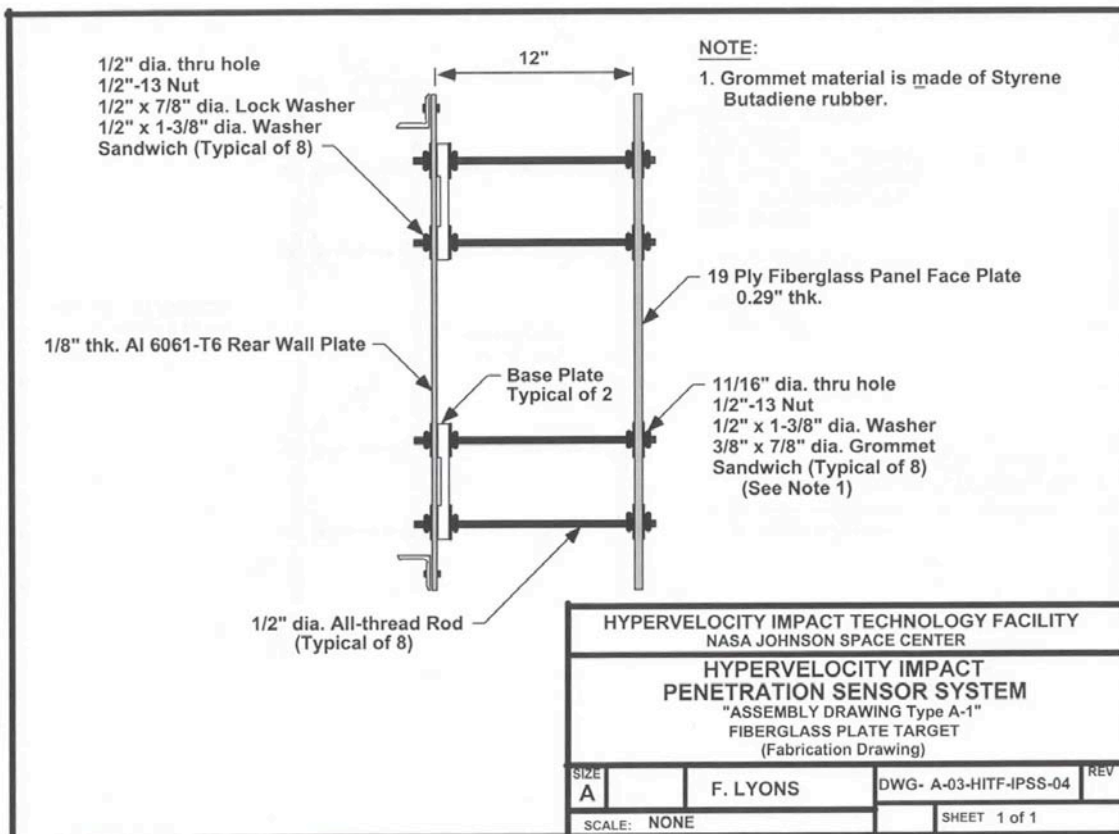


Figure 2: Target A-1 Drawing

Target A-2 (Figure 3 and Figure 4) was similar to Target A-1 but the fiberglass panel was not isolated from the all-thread (no grommets).

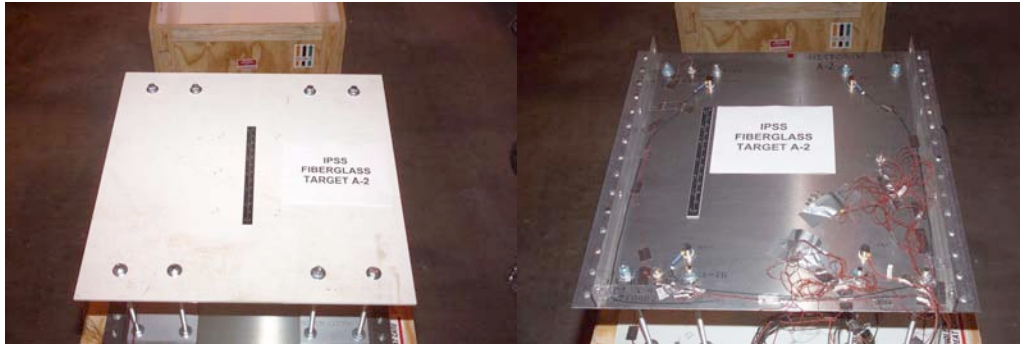


Figure 3: Target A-2 Left: Top View. Right: Bottom View.

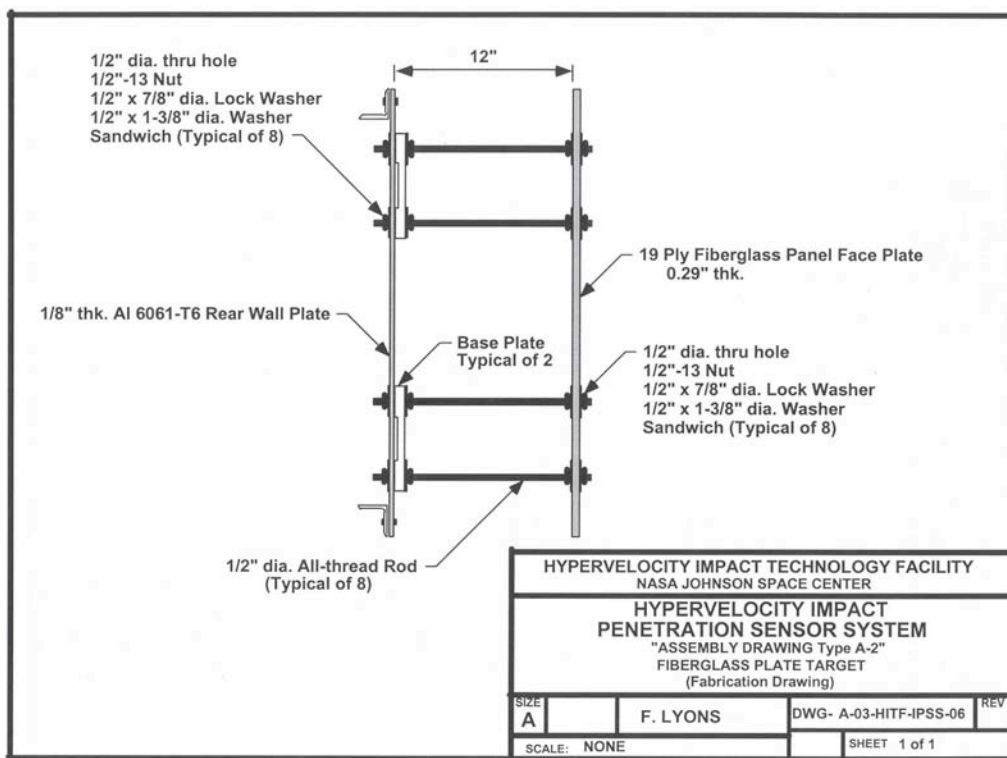


Figure 4: Target A-2 Drawing

Target B-1 (Figure 5 and Figure 6) used two fiberglass plates to model MMOD impacts with a trajectory that would go through the WLE panel and not intersect directly with the wing spar. Target B-1 consisted of a 30 x 30 19 ply fiberglass panel, a 12" gap, a second 19 ply fiberglass panel, a 3.8" gap, and a 0.125" thick aluminum plate. Target B-1 contained grommets that isolated the fiberglass panel from the 0.5" all-thread.

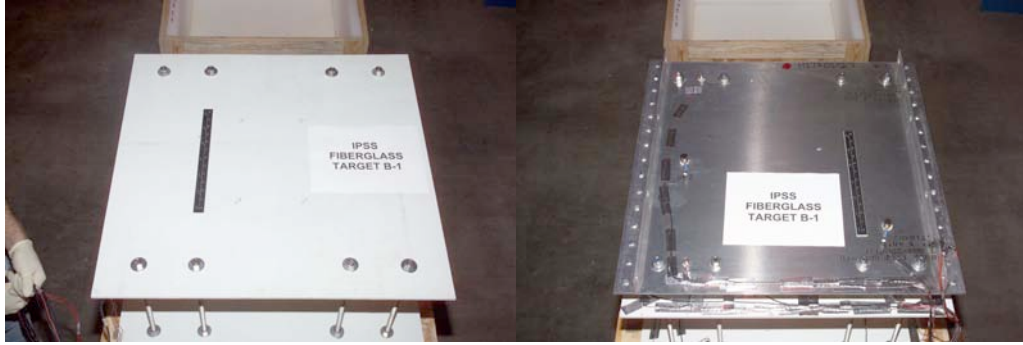


Figure 5: Target B-1. Left: Top View. Right: Bottom View.

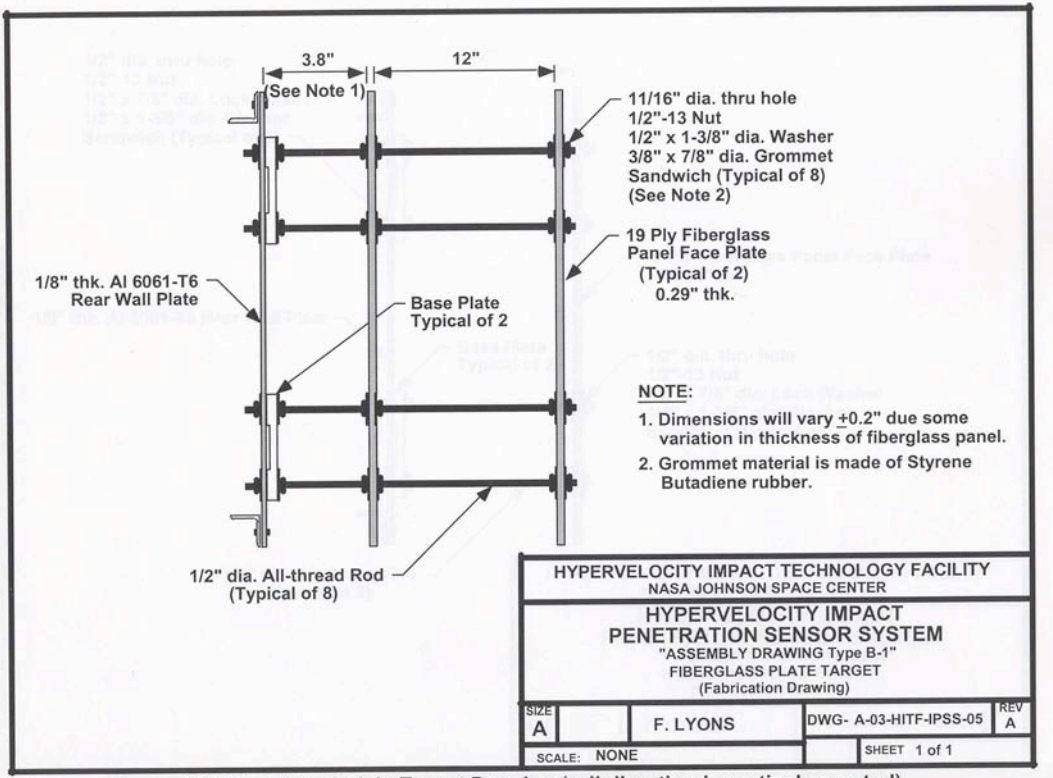


Figure 6: Target B-1 Drawing

There were a total of 15 shots fired. All targets were oriented at 90 degrees (perpendicular to gun bore) for all shots (Figure 7).

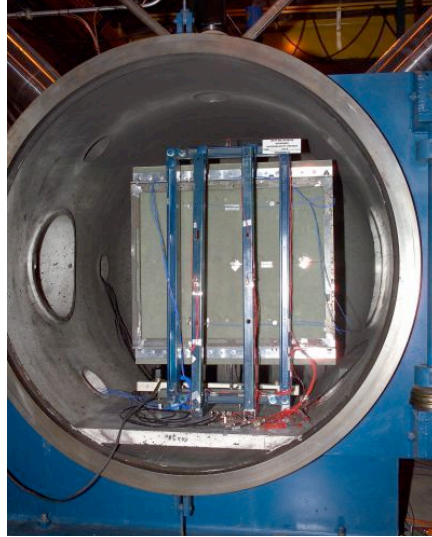


Figure 7: Fiberglass Panel Target with 90 deg Impact Angle. Back Side View.

The tests were conducted on the 0.50 caliber hypervelocity launcher range at the White Sands Test Facility (WSTF). The flight range for the hypervelocity projectile and target chamber were evacuated to near vacuum pressure (6-8 Torr) prior to each shot. The AE recording equipment was connected by feed-throughs to the sensors on the target inside the vacuum chamber. The connectors were BNC type.

The projectiles were small spheres made of 2017 T-4 aluminum. They ranged in diameter from 0.4 mm to 5.6 mm. Impact velocity was measured with WSTF diagnostic equipment on each shot. The projectile kinetic energy for these shots ranged from 2.01 J to 7164.18 J.

On Targets A-1 and A-2, four acoustic (ultrasonic) emission sensors were coupled to the aluminum backplate with Lord 202 acrylic adhesive (Figure 8). Two sensors were coupled to the surface of the fiberglass panel. Diagrams of the sensor layout are shown in Figure 9, Figure 10, Figure 11, and Figure 12.

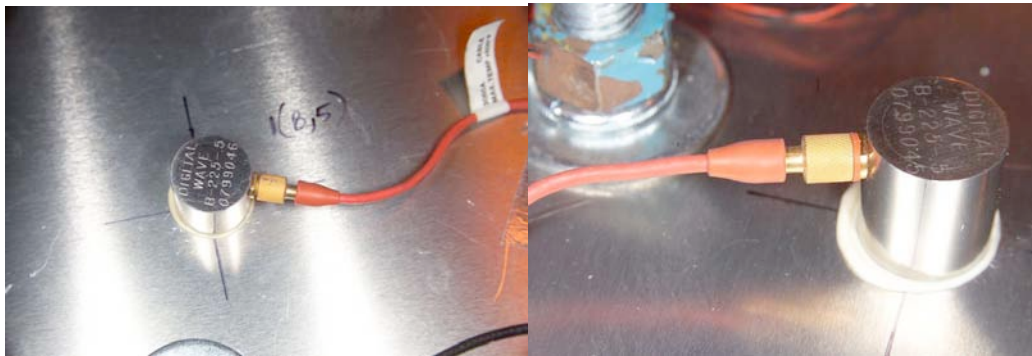


Figure 8: Detail of Sensors on Targets A-1 (left) and A-2 (right).

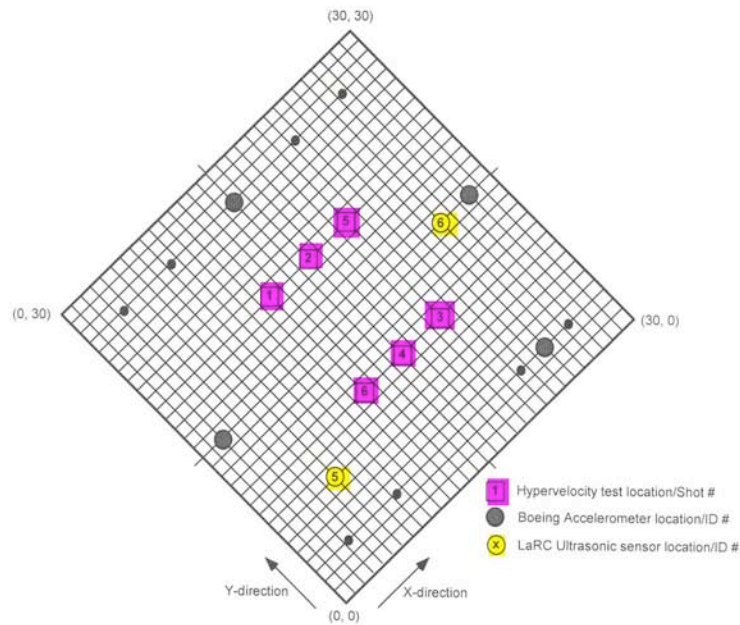


Figure 9: Diagram of Sensor Locations on Fiberglass Panel Target A-1. Front View. Acoustic emission sensors are highlighted in yellow with the following coordinates: #5(6, 7), #6 (25, 15) Dimensions are inches. Impact locations are highlighted in magenta with the following coordinates: #1 (12, 20), #2 (16, 20), #3 (20, 10), #4 (16, 10), #5 (20, 20), #6 (12, 10)

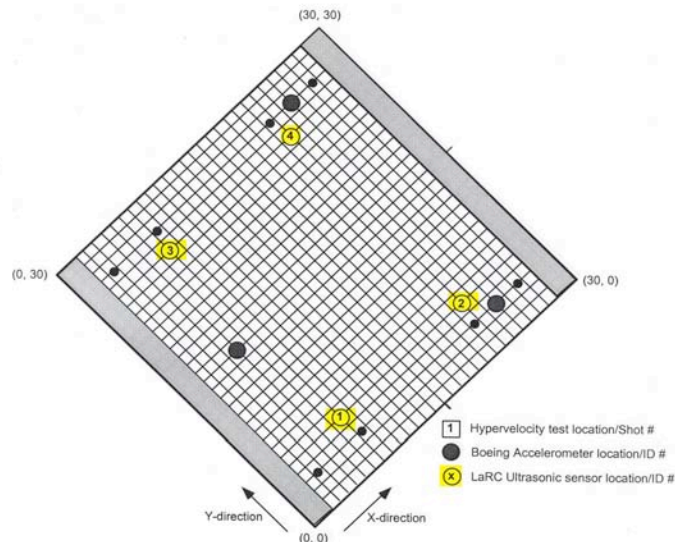


Figure 10: Diagram of Sensor Locations on Aluminum Back Plate Target A-1. Front View. Acoustic emission sensors are highlighted in yellow with the following coordinates: #1 (8, 5), #2 (22, 5), #3(8, 25), #4 (22, 25) Dimensions are inches.

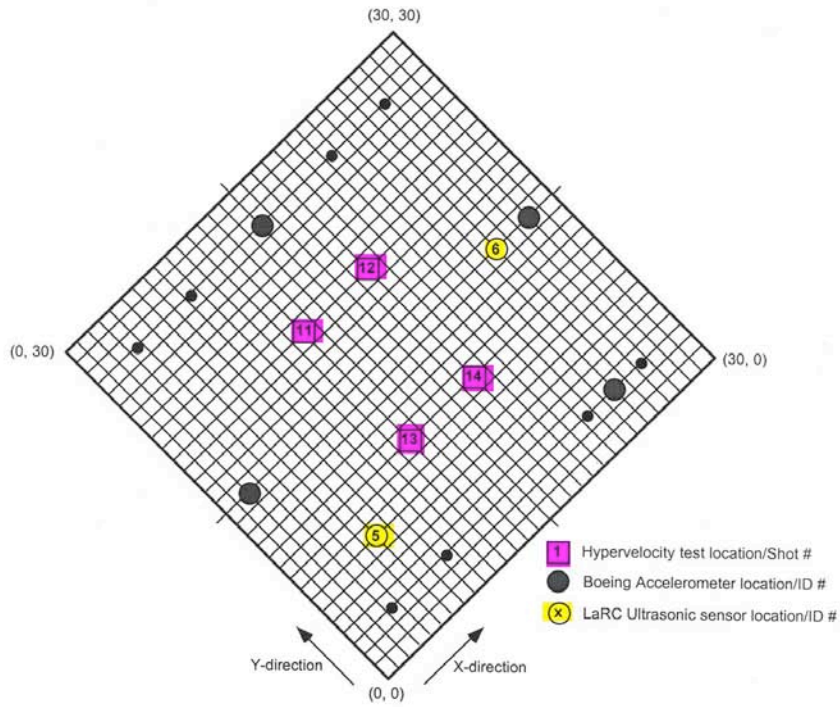


Figure 11: Diagram of Sensor Locations on Fiberglass Panel Target A-2. Front View.
 Acoustic emission sensors are highlighted in yellow with the following coordinates:
 #5(6, 7), #6 (25, 15) Dimensions are inches.
 Impact locations are highlighted in magenta with the following coordinates:
 #11 (12, 20), #12 (12, 10), #13 (18, 20), #14 (18, 10), #15 (20, 20)

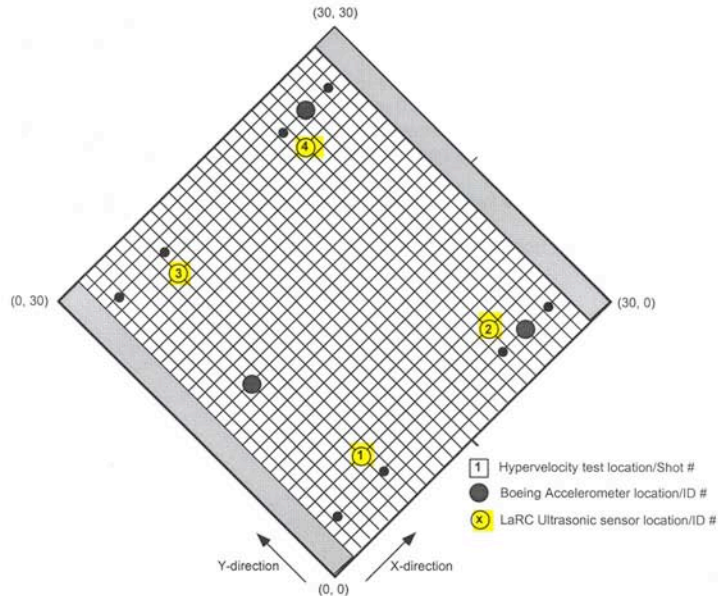


Figure 12: Diagram of Sensor Locations on Aluminum Back Plate Target A-2. Front View.
 Acoustic emission sensors are highlighted in yellow with the following coordinates:
 #1(8, 5), #2(22, 5), #3(8, 25), #4 (22, 25) Dimensions are inches.

On Target B-1, sensors 1-4 were coupled to the second fiberglass plate with Lord 202 acrylic adhesive. Sensors 5 and 6 were coupled to the first fiberglass plate and sensors 7 and 8 were coupled to the aluminum backplate. Diagrams of the sensor layout are shown in Figure 13, Figure 14, and Figure 15.

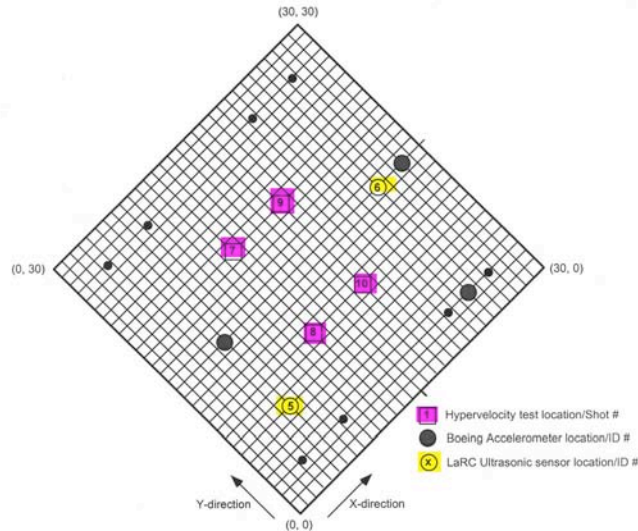


Figure 13: Diagram of Sensor Locations on Fiberglass Plate 1 Target B-1. Front View.
 Acoustic emission sensors are highlighted in yellow with the following coordinates:
 #5(6, 7), #6 (25, 15) Dimensions are inches.
 Impact locations are highlighted in magenta with the following coordinates:
 #7 (12, 20), #8 (12, 10), #9 (18, 20), #10 (18, 10),

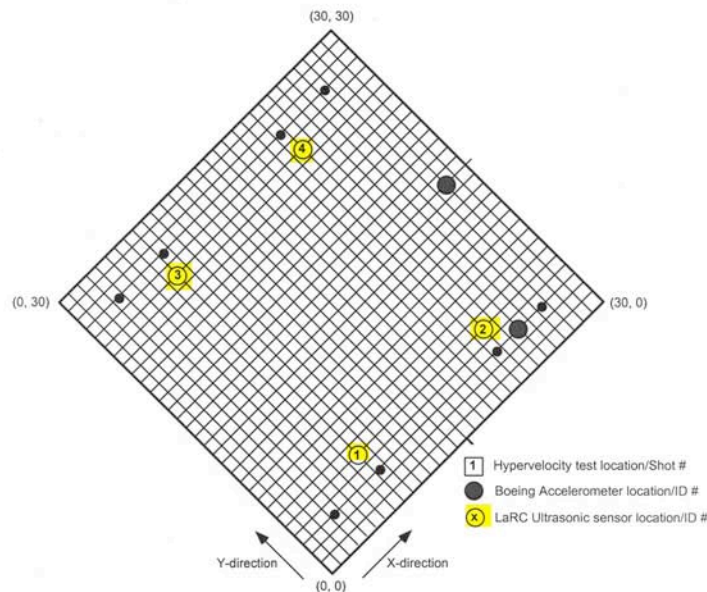


Figure 14: Diagram of Sensor Locations on Fiberglass Plate 2 Target B-1. Front View.
 Acoustic emission sensors are highlighted in yellow with the following coordinates:
 #1 (8, 5), #2 (22, 5), #3 (8, 25), #4 (25, 15) Dimensions are inches.

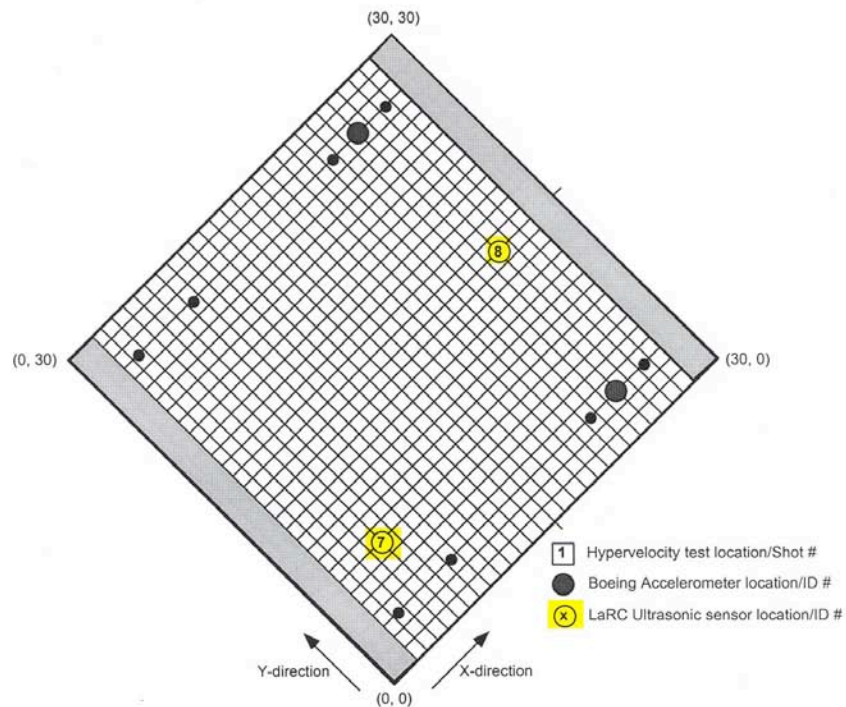


Figure 15: Diagram of Sensor Locations on Aluminum Back Plate Target B-1. Front View.
Acoustic emission sensors are highlighted in yellow with the following coordinates:
#7(6, 7), #8 (25, 15) Dimensions are inches.

The piezoelectric sensor converted the sound wave energy to an electrical voltage. The energy computed from the voltage data collected by each sensor channel is referred to as the wave signal energy. (A complete description of the type of sensor used and calibration is given in the General Introduction to this report.)

The wave signal energy for each channel was analyzed and compared to the impact energy. A full description of the wave recording instrumentation is given in the General Introduction to this report. (Each individual sensor was connected to a separate amplification and filtering channel and the voltage produced by the sensor recorded and stored on a computer.)

The wave signal energy was computed by integrating the squared voltage with respect to time and dividing this number by the impedance at the preamp input. The voltage versus time values of the wave, which were displayed in the waveform window on the computer screen for each channel, were corrected for any applied gain (or attenuation).

Attenuation was the norm because hypervelocity impact produced very energetic signals that in most cases would have saturated the A/D converter on the recording card in the computer had the amplitude not been reduced.

Some recorder channels were found to have a slight DC offset (Figure 16). This added significantly to the wave energy when the integral of squared voltage versus time signal was computed. To eliminate the offset, the average wave signal voltage for the impact event was subtracted from each data point. This resulted in a zeroed raw wave signal (no DC offset). Correcting the offset was more important for small signals than large signals.

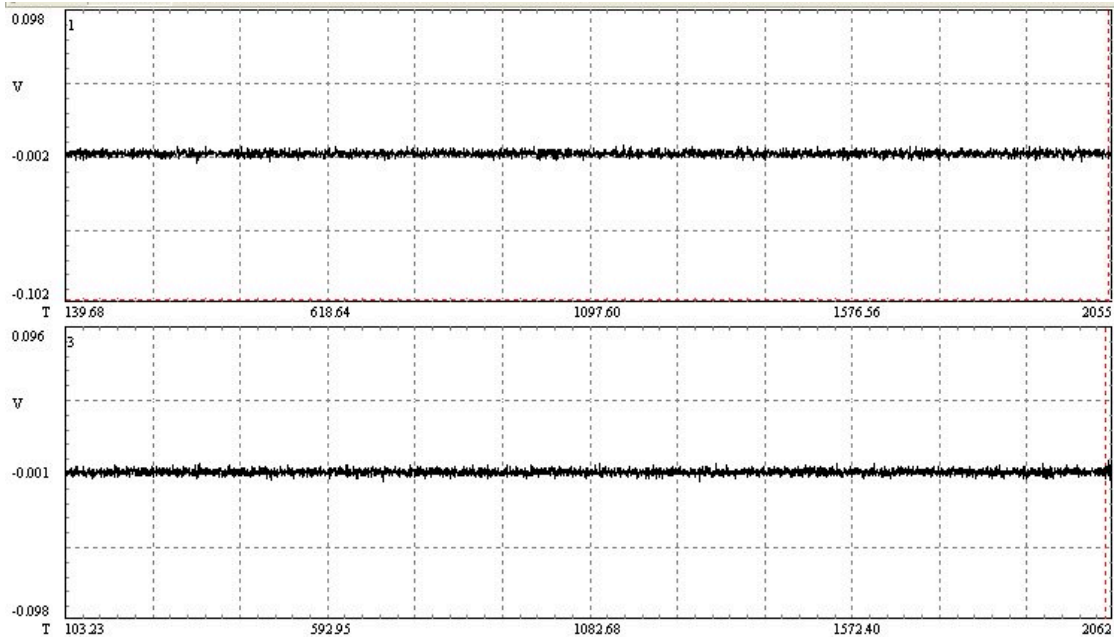


Figure 16: Example of DC Offset

The top signal is centered at -0.002 V whereas the bottom signal is centered at -0.001V.

A typical impact signal is shown in Figure 17. The impact signal has a distinct waveform and varies in both in arrival time and amplitude on each channel. The distinct modal characteristics can be seen in a time expanded view in Figure 18. The E mode is seen to arrive first with its lowest frequency in front followed by progressively higher frequencies. This is followed by the flexural (F) wave. The F wave characteristics are harder to discern because of the filtering of the attenuators and other effects that tended to damp out the low frequencies.

The propagation through the standoffs and secondary particles distorted the signal. In some cases, the F wave characteristics were much more visible. The vastly different velocities of the modes were used to confirm the modes' presence.

The sound waves produced by each impact are shown complete in the Appendix to this section. There it can be seen that the impact waves have the plate mode characteristics, i.e., the extensional wave arrives first, with its low frequency components out front followed by higher frequency components, and the F wave with just the opposite frequency arrangement. This differs, for example, from noise caused by electromagnetic interference (EMI). In contrast, EMI noise typically looks the same on every channel and

arrives simultaneously (Figure 19). EMI exhibits no plate wave propagation characteristics.

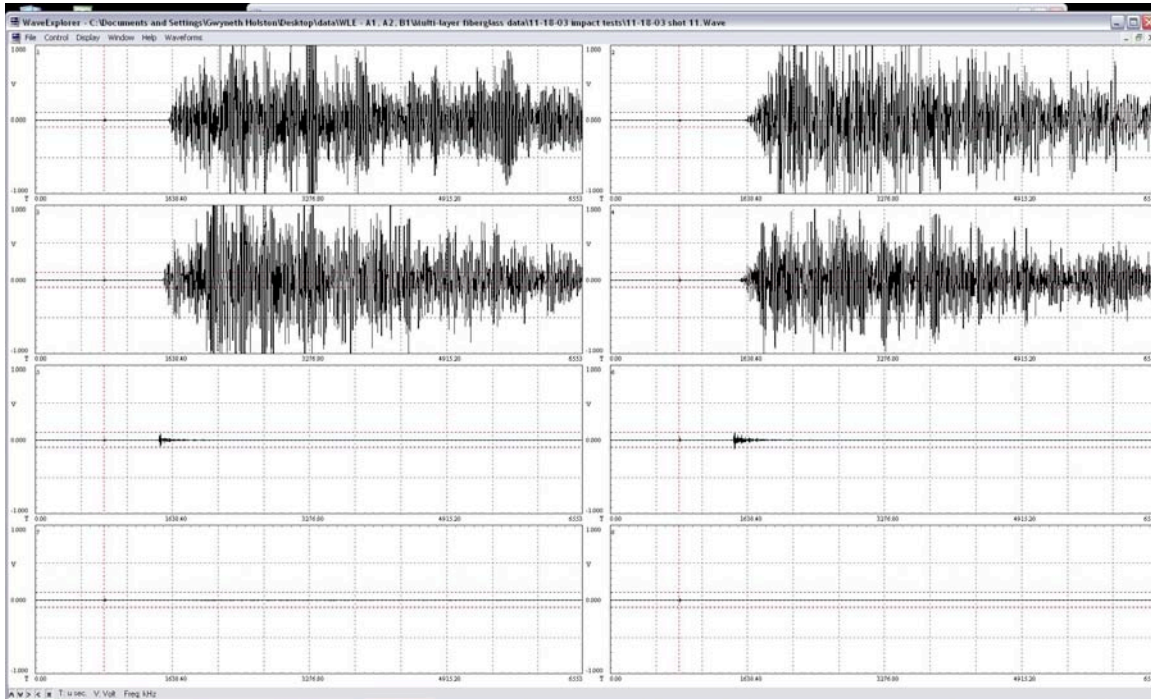


Figure 17: A-2 Impact Signal for Shot #11

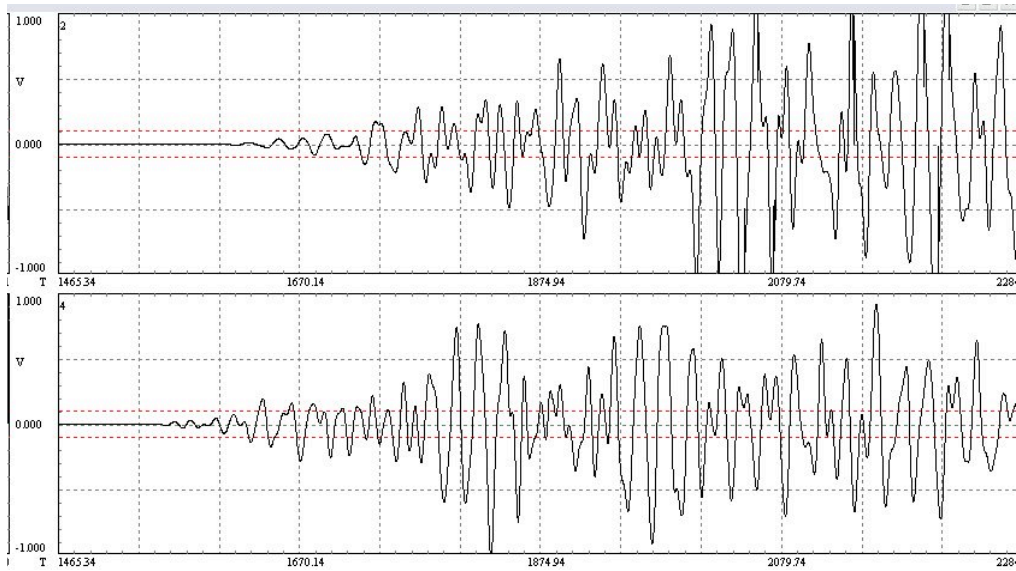


Figure 18: Detail of A-2 Impact Signal for Shot #11, Sensors 2 and 4

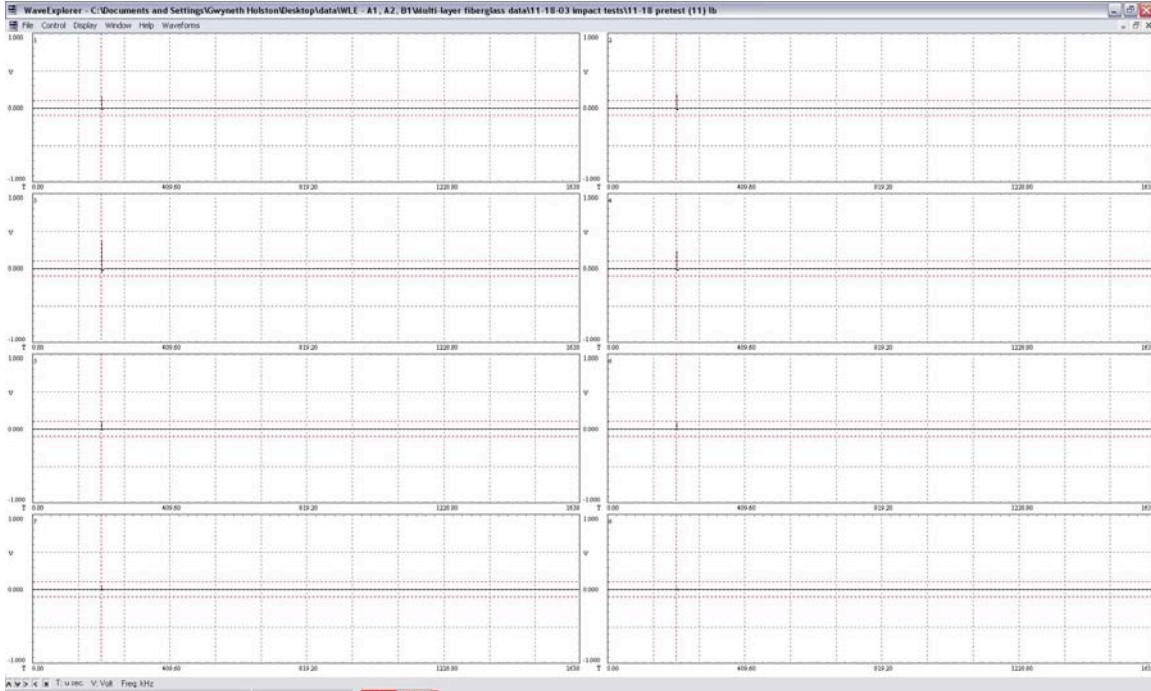


Figure 19: A-2 Electromagnetic Interference for Shot #11

The MAE software computed the raw wave signal energy in Joules uncorrected for any analog gain or attenuation that may have been applied to the signal path. In order to compare the wave energies from shot to shot, the raw wave signal energy is converted by applying Equation 1 where E_{raw} is the energy computed using the recorded wave (with DC offset eliminated) and G is the system gain.

$$W.S.E. = \frac{E_{raw}}{G^2} \quad \text{Equation 1}$$

The gain G is computed by converting the logarithmic gain, M , in decibels with Equation 2 or 3.

$$M \text{ dB} = 20 \text{ Log}_{10} (G) \quad \text{Equation 2}$$

$$G = 10^{\frac{M}{20}} \quad \text{Equation 3}$$

The gains, raw wave signals, and wave energies for each shot are listed in the data tables in the Appendix to this section.

High velocity impact produced signals on the order of a few volts directly out of the transducer. These were much larger signals than typically found in most acoustic emission measurements of, say, crack growth in metals. For most shots, attenuators were

placed in the signal lines between the sensors and the digital recorders. Greater attenuation was applied for the higher energy shots which made the raw energy appear to be much less. The energy was restored to its full value by compensating in the analysis for the greater attenuation, Equation 3 above.

Results

The most important quantities used in the analysis of the wave signals were the wave signal energy and projectile kinetic energy for each shot. These are given in Table 1 along with the test number and impactor diameter. Wave signal energy is the sum of the energy, in Joules, detected by all of the sensors. Kinetic energy is calculated based on the velocity and mass of projectile (density of aluminum = 2700 kg/m³) according to the usual formula $K.E. = mv^2/2$. As will be seen, the kinetic energy correlated fairly well with the damage. Normal KE is just the kinetic energy associated with the projectile velocity component normal to the target surface at the point of impact.

Test No.	Imp Dia mm	Kinetic Energy J	W.S.E. nJ
A1-1	1.0	31.83	3.836E+01
A1-2	1.4	87.59	1.262E+03
A1-3	1.6	128.81	1.915E-01
A1-4			
A1-5	5.6	5841.76	9.453E+03
A1-6	6.0	7101.57	6.447E+03
B1-7	1.6	134.67	3.168E+05
B1-8	2.0	257.65	2.276E+03
B1-9	5.6	6013.32	2.904E+04
B1-10	6.0	7164.18	3.723E+04
A2-11	1.0	31.92	2.096E+02
A2-12	1.4	85.00	1.032E+03
A2-13	1.6	129.58	3.345E+03
A2-14	2.0	257.65	4.958E+03
A2-15	0.4	2.01	2.548E+00

Table 1: Kinetic Energy and Wave Signal Energy for Fiberglass Panel Target A-1, B-1, and A-2.
No data was available for shot #4.

The damage for each shot is given in Table 2. The crater volume damage is the product of the recorded length, width, and depth measurements on the front side of the panel for each impact. Damage area is the product of recorded length and width measurements on the front side of the panel. Examples of impact damage are Figure 20, Figure 21, and Figure 22.

Test No.	Kinetic Energy J	Crater Volume mm ³	Damage Area mm ²
A1-1	31.83	126.0	80.0
A1-2	87.59	225.0	229.5
A1-3	128.81	643.5	208.0
A1-4		1244.9*	513.0
A1-5	5841.76	2386.6*	513.0
A1-6	7101.57	4235.5*	89900.0
B1-7	134.67	180.0	289.0

Table 2: Damage Results for Fiberglass Panel Targets A-1, B-1 and A-2.

* = Hole. No kinetic energy data was available for shot #4

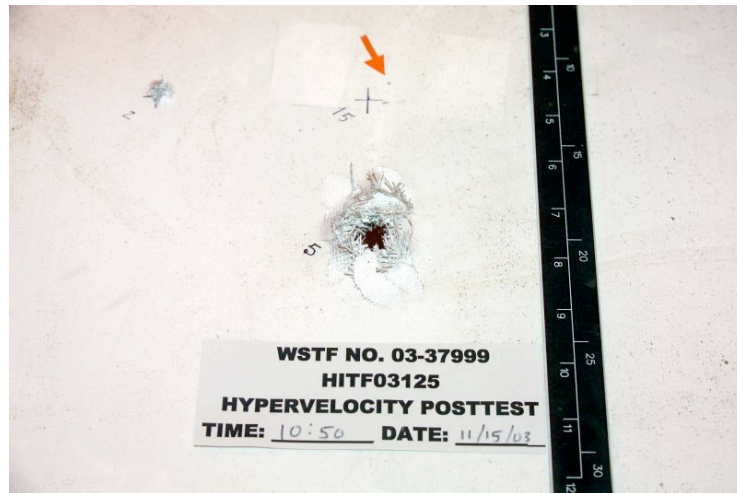


Figure 20: A-1 Shot #5 Impact Damage

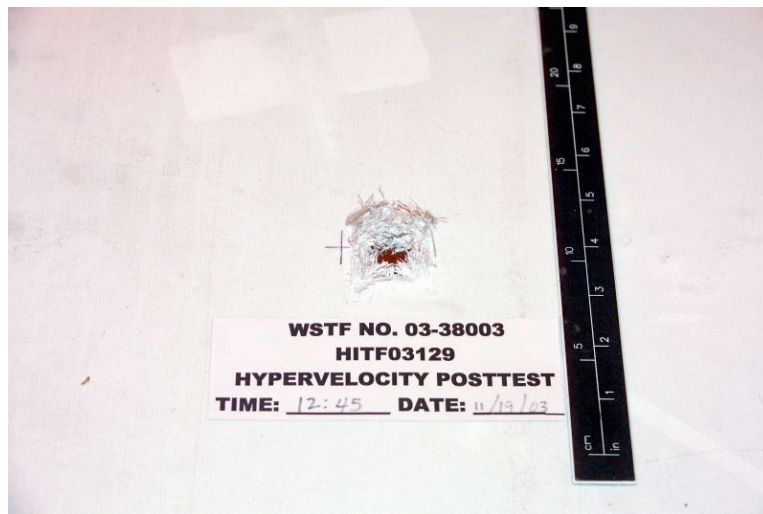


Figure 21: B-1 Shot #10 Impact Damage

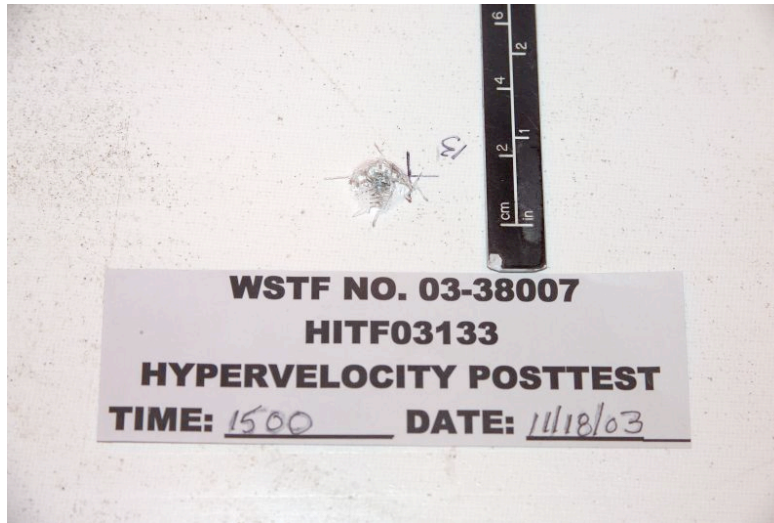


Figure 22: A-2 Shot #13 Impact Damage

Discussion

Comparing multi-layer targets was challenging due to the difference in construction of each target. Sensors 5 and 6 on the front fiberglass plate of each target picked up the largest wave signal energies. Energy from the front plate was then transmitted along the all-thread aluminum rods to the next plate. Targets A-1 and B-1 had grommets to insulate the rods from the fiberglass unlike Target A-2 second plate data. Targets A-1 and B-1 were not directly compared to each other because the second plate in A-1 is an aluminum back plate whereas the second plate in B-1 is fiberglass. Aluminum and fiberglass have different wave propagation properties. More testing is required to draw significant conclusions for each individual target.

For these targets, after the impactor hit the first layer of fiberglass, small particles impacted the second layer of fiberglass (Figure 23). This is referred to as 'spalling damage'. The secondary impacts reflected back up the metal rods that joined the layers together resulting complex data recorded by sensors on the first layer. The time for collecting wave signal energy was approximately 1000 μ s after impact. This very short time may have only collected the energy due to the primary impact on the first layer of fiberglass, but it may have also measured some of the energy from the spall. This should be kept in mind as an additional source of possible error.

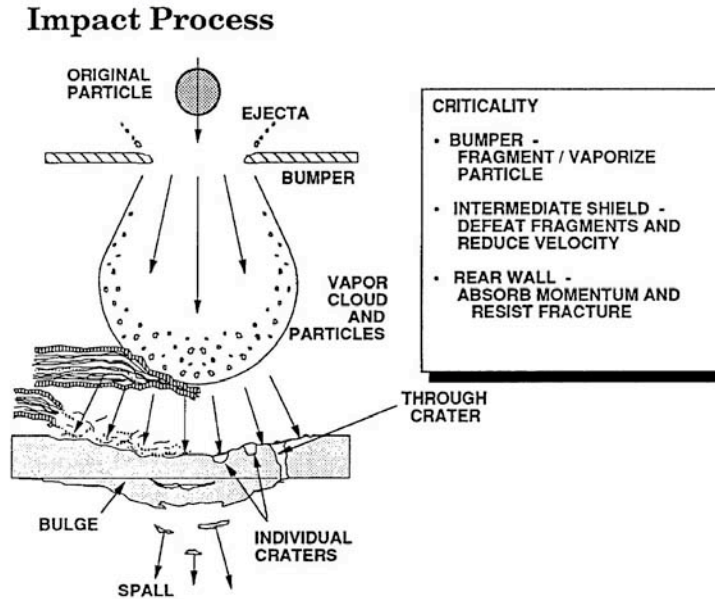


Figure 23: Multilayer Penetration Mechanisms¹

Only two sensors were located on each front fiberglass plate. This made it difficult to collect a consistent fraction of the energy transmitted into the plate. If sensors surrounded the impacts, one could add the wave signal energy collected by each sensor to obtain the total wave signal energy. Two symmetric impacts would have symmetric propagation paths and thus the same total wave signal energy when the energy collected by all the sensors are summed. This technique was useful for all other targets (C-1, C-2, Fg(RCC)-1, Fg(RCC)-2, RCC16R) because each had at least four sensors that surrounded the impacts. Since A-1, B-1, and A-2 had only two sensors located on the front fiberglass plate, impacts with similar kinetic energy yielded varying amounts of wave signal energy depending upon their proximity to the sensors.

Target A-1

Sensors 5 and 6 were affixed to the fiberglass panel of Target A-1 (Figure 9). Sensors 1-4 were affixed to the aluminum backplate (Figure 10). Shots #1- 6 struck Target A-1. Shots #5 and #6 created holes rather than craters. There were a variety of data acquisition problems for shots #1, 3, 4, 5, and 6.

Selecting the amount of gain or attenuation for these shots was an iterative process since it had not been done before.

There was too much attenuation on shot #1, channels 5 and 6 (see Figure 24). Channel 5 showed a very small signal that was later traced to a bad preamp input connector.

¹ Figure 3-1 Multi-layer penetration mechanisms. "Structural Damage Prediction and Analysis for Hypervelocity Impacts – Handbook" p. 3-9 N.C. Elfer, 1996

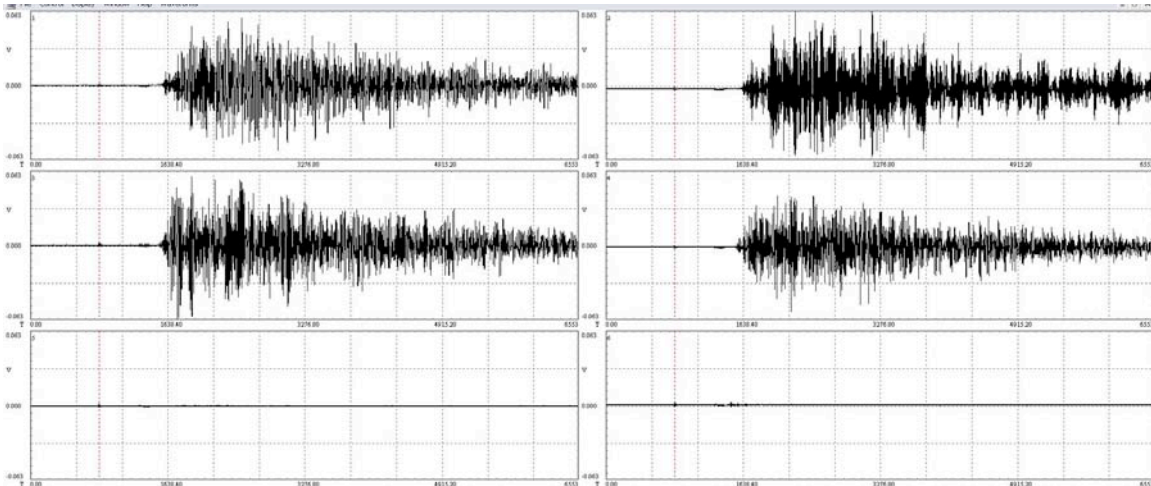


Figure 24: Impact Waveform for Shot #1. Notice the missing signal for sensor 5 in the bottom left corner.

There was some saturation on sensor 2 for shot #3 and sensor 5 signals were not acquired because of the bad preamp input connector.

No data was available for shot #4.

The gain was too high on channels 1-4 on shot #5 causing saturation (Figure 25). Large EMI signals were observed on all channels at and just after trigger. Sensors 2 and 6 were knocked off of the specimen and had to be rebonded before the next test.

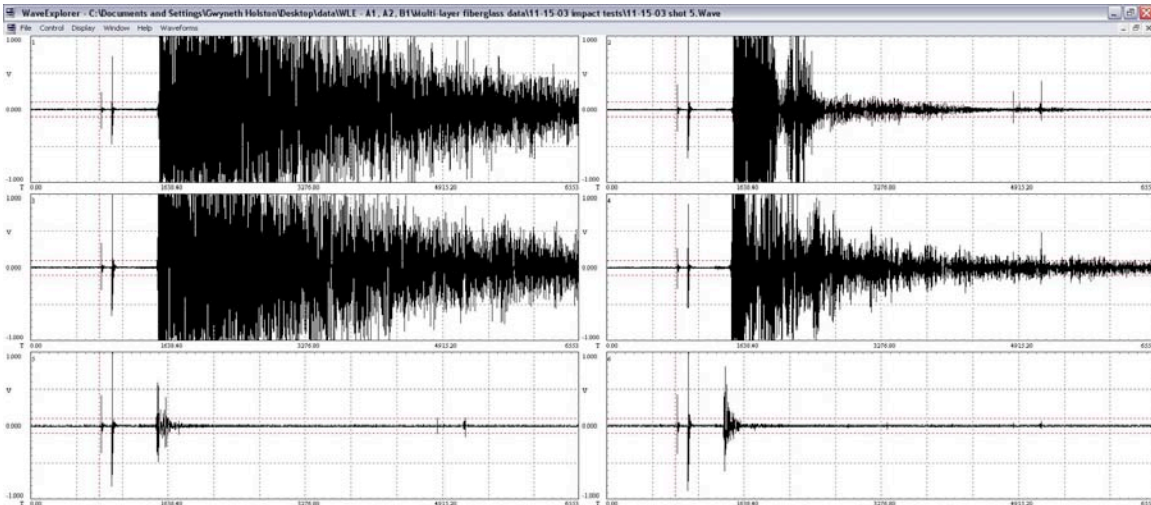


Figure 25: Shot #5 Impact Waveform. Notice saturation on channels 1-4. Channels 2 and 6 have shortened signals due to sensors being knocked off during impact.

On shot #6, sensor 1 was knocked off of the specimen during impact.

Good data was collected on Target A-1 fiberglass plate sensors 5 and 6 for shots #2, 5, and 6. Predictably, the shots with high kinetic energies (shots #5 and 6) created holes and also had high wave signal energies.

Good data was collected on Target A-1 aluminum back plate sensors 1-4 only for shot #2.

Target A-2

Like A-1, sensors 5 and 6 were affixed to the fiberglass panel on Target A-2 (Figure 11). Sensors 1-4 were affixed to the aluminum backplate (Figure 12). Shots #11- 15 struck target A-2. Only shot #14 created a hole. There were data acquisition problems for shots #11, 12, and 15.

Signals saturated on channels 1-3 for shot #11. Shots #12 and #15 suffered from the aforementioned bad preamp input connector on sensor 5.

Acceptable data was collected on Target A-2 fiberglass plate sensors 5 and 6 for shots #11, 13, and 14. The wave signal energy for these shots was plotted versus kinetic energy in Figure 26. There was a trend of increasing wave signal energy with increasing kinetic energy.

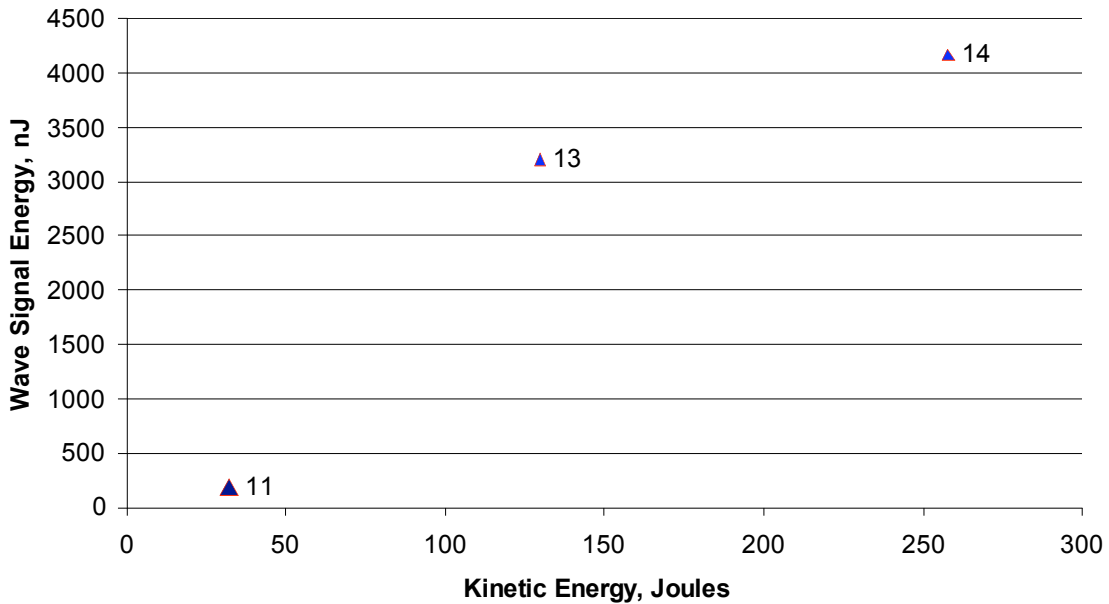


Figure 26: Wave Signal Energy vs. Kinetic Energy on A-2 Fiberglass Plate (Sensors 5 and 6)

Good data was collected on Target A-2 aluminum back plate sensors 1-4 for shots #12- 15. The wave signal energy versus kinetic energy shows a linear trend in Figure 27. Shot #14 created a hole and had a high wave signal energy.

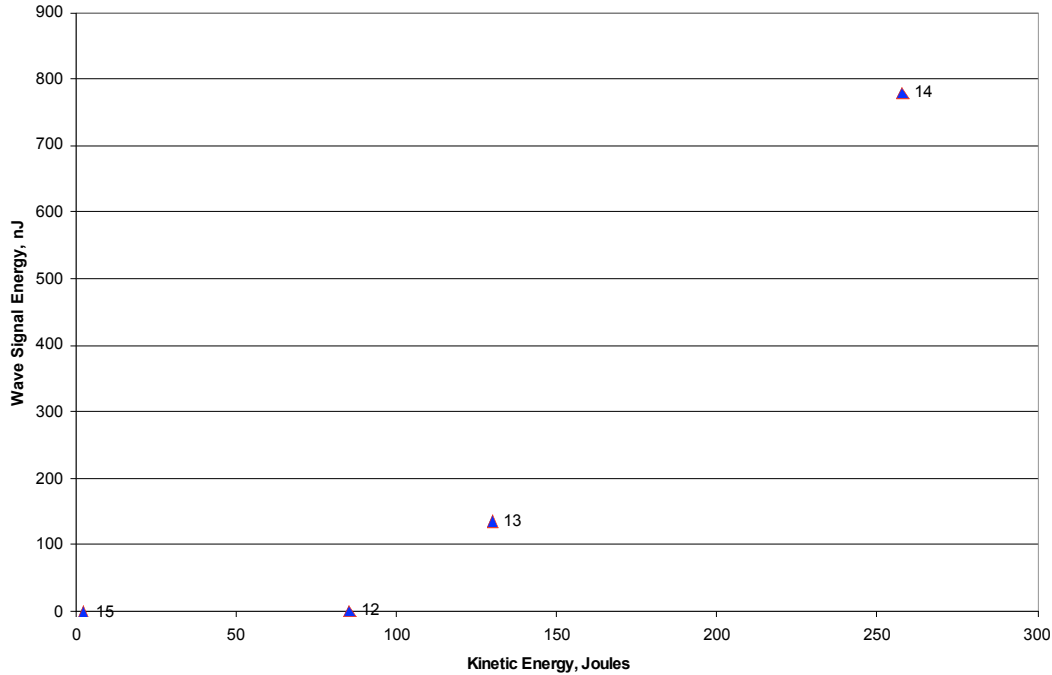


Figure 27: Wave Signal Energy vs. Kinetic Energy for A-2 Aluminum Back Plate (Sensors 1-4)

The purpose of Targets A-1 and A-2 was to compare the effect that grommets had on signals recorded by sensors on the aluminum back plate. Shots #12 (Target A-2) and #2 (Target A-1) had similar kinetic energies and similar wave signal energies on front panel sensors 5 and 6. The difference in wave signal energies on the back plate due to the existence of grommets was ~14 dB. This was confirmed by shots #13 and 3.

Target B-1

Sensors 5 and 6 were affixed to fiberglass plate 1 on Target B-1 (Figure 13). Sensors 1-4 were affixed to fiberglass panel 2 (Figure 14). Sensors 7 and 8 were affixed for the aluminum back plate (Figure 15). Shots #7-10 struck target B-1. Shots #9 and 10 created holes. There were data acquisition problems for shots #7, 9, and 10.

Signals were not acquired for shot #7 on channel 5 due to the aforementioned bad preamp connector. The gain setting on channel 6 of shot #7 was questionable. Shots #3 and 7 had very similar kinetic energies and similar raw wave signals on sensors 6. The calculated wave signal energy (Equation 1, p. 17 and Table 7, p. 64), however, was a million times larger for shot #7 than shot #3 due to gain settings of -64 dB and -50 dB, respectively. By comparing the raw signals (Figure 28), it was concluded that the gain for shot #7 must be relatively close to the gain for shot #3, (-50 dB rather than the data sheet value of -64 dB). If the gain on shot #7 were indeed -64 dB, its raw wave signal (Figure 28) should have appeared at least four times larger than the signal for shot #3.

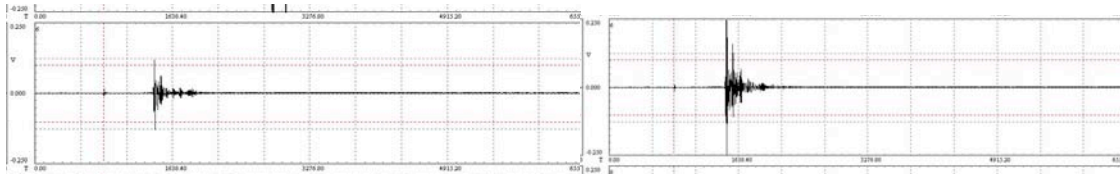


Figure 28: Shot #3 Impact Waveform, Sensor 6 (left) and Shot #7 Impact Waveform, Sensor 6 (right)

Shot #9 was barely saturated on channel 4. There was too much attenuation on channels 7 and 8. Sensor 6 became disbonded as was evident in signal (Figure 29). Sensor 6 was tested and replaced for the next shot.

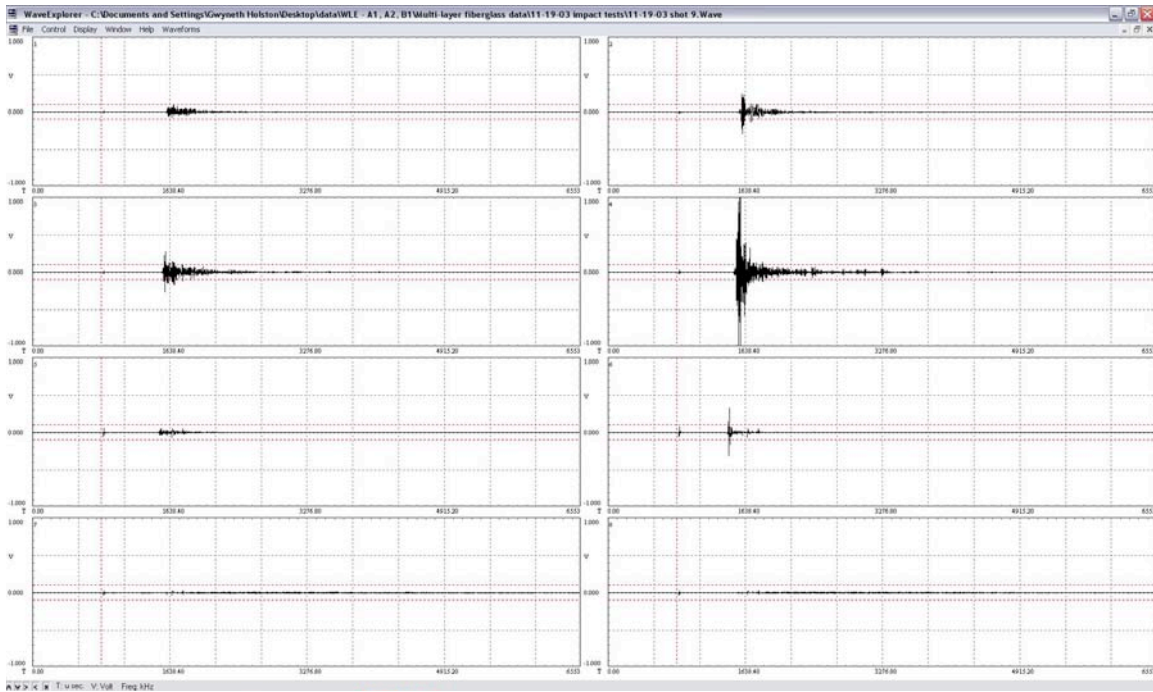


Figure 29: Shot #9 Impact Waveform

Shot #10 was slightly saturated on channels 7 and 8 (Figure 30).

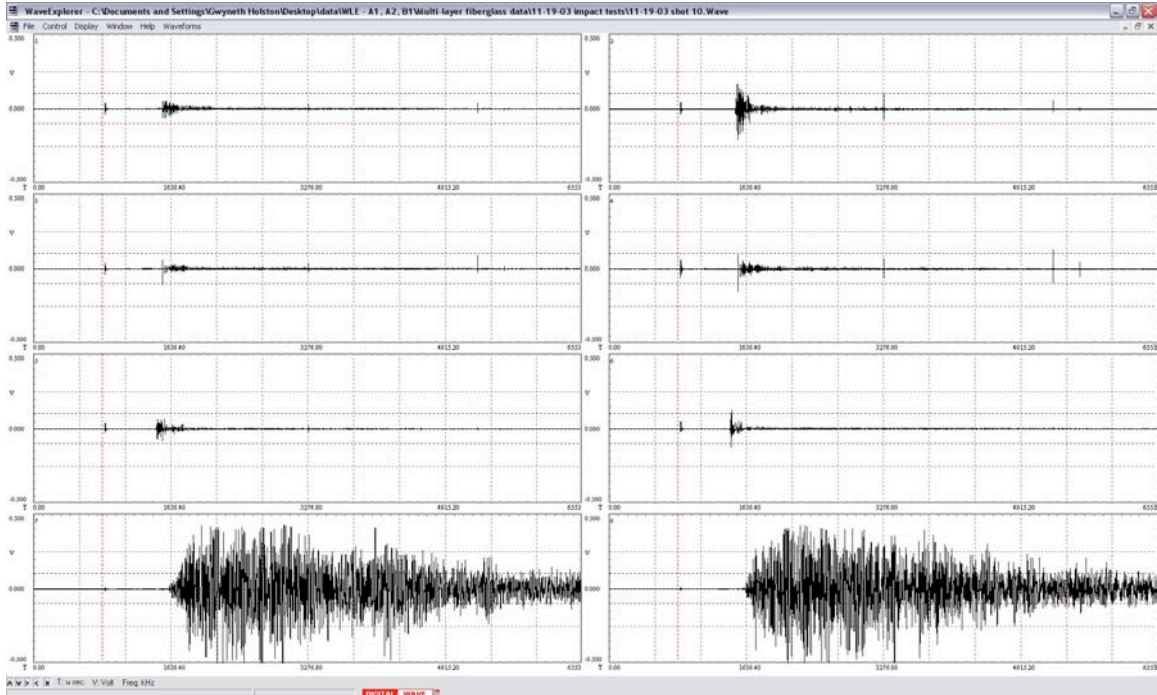


Figure 30: Shot #10 Impact Waveform

Acceptable data was collected on Target B-1 fiberglass plate 1 sensors 5 and 6 for shots #8 and 10. Shot #10 created a hole and had both a higher kinetic energy and wave signal energy than shot #8.

Good data was collected on Target B-1 fiberglass plate 2 sensors 1-4 for shots #7, 8, and 10. All three shots were in keeping with the trend of increasing wave signal energy with increasing kinetic energy.

Valid data was collected on Target B-1 aluminum back plate sensors 7 and 8 for shots #7 and 8. Consider the impact waveform for shot #7 (Figure 31). The wave signal first arrived on sensors 5 and 6 since they were located on the first layer of fiberglass. It arrived at sensor 5 slightly before sensor 6 because it impacted closer to sensor 5. These channels clearly showed a large amplitude at initial impact that decreases with time. The wave signal then proceeded to sensors 1-4 on the second layer of fiberglass. The wave signal appears distorted because it had to travel through the all-thread rods from the first fiberglass plate to the second. The wave reverberated inside the rods to create the types of signals observed on sensors 1-4 and, finally, 7 and 8.

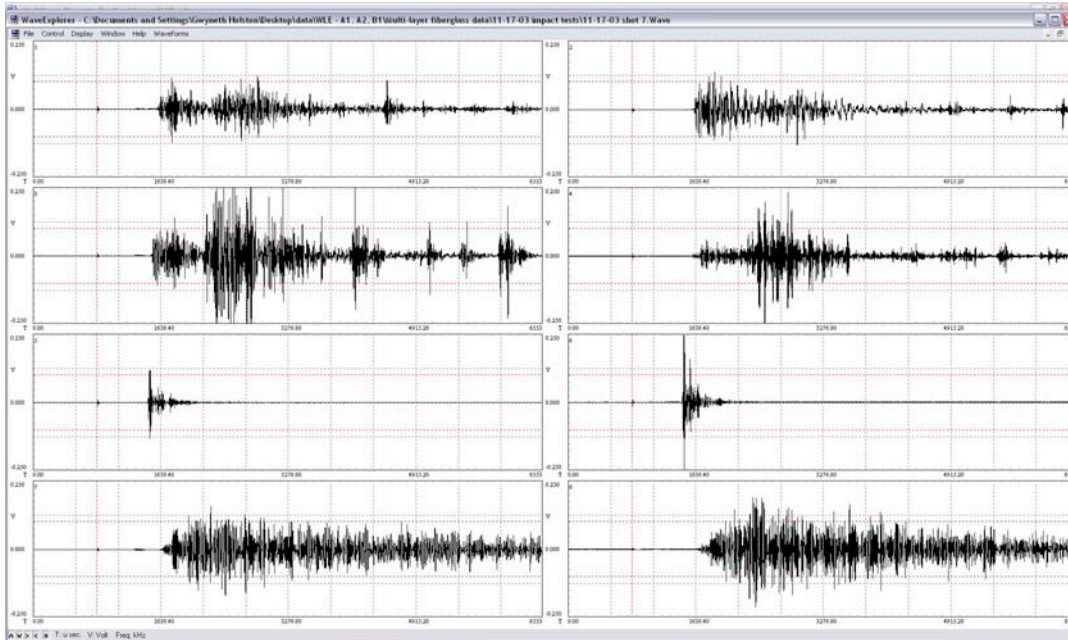


Figure 31: Shot #7 Impact Waveform, Sensors 1-8

Location Analysis

Location of the source of a wave is part and parcel of the MAE technique just as it is in SONAR methods. It contributes to understanding the type and magnitude of the source and is a crucial step in tracking down and stopping leaks in manned spacecraft.

In these studies the location of the impact was known by visual observation. This enabled a study of the accuracy of locating a source purely by analysis of the wave arrival at different transducers. The source position was triangulated when the source to receiver path was reasonably homogeneous. This was shown in detail for Target Fg(RCC)-1 and the reader is referred to that Section of this Report.

The velocities of the direct arrivals were measured in advance. Pencil lead breaks were done to create the modes. This is discussed under the section on Wave Propagation below.

Wave Propagation

The wave signal energy collected by any given sensor is composed of direct energy and reflected energy. After an impact occurs, a wave propagates radially outward from the impact site. This direct wave is the first signal recorded by a sensor. When this wave reaches the edges of the target, it is reflected back to the sensor. These reflected waves are lower in amplitude than the direct waves and have later arrival times. In general, reflected waves did not contribute not a significant fraction of the signal energy.

The direct wave is composed of two types of waves: extensional and flexural. Extensional waves have two displacements components with the larger displacements perpendicular to the normal to the plate. A sensor on the surface detects the out-of-plane component of the E wave. The largest displacement of the flexural wave motion is perpendicular to the plane of the plate. This motion is caused by bending at the impact location. The E and F modes have very distinct characteristics (see General Introduction) that can be readily identified. For one thing, the front part of the E wave travels much faster than any frequency component of the F wave.

Wave speed was determined by performing a lead break at one sensor and measuring the time it takes for a direct wave to arrive at another sensor at a known distance away. Except for the second fiberglass plate of B-1, there were only two sensors on each fiberglass plate. This means that the wave speed could only be calculated in one direction. Fortunately, the speeds of extensional and flexural waves were already calculated for Targets C-1 and C-2. Extensional waves traveled 0.16 in/ μ s in the x-direction, 0.16 in/ μ s in the y-direction and 0.14 in/ μ s in the diagonal. Flexural waves traveled 0.06 in/ μ s in all directions.

In the fiberglass panel, fibers are aligned in the x and y directions (see Figure 9). In addition to having slower speeds, waves that travel diagonally are attenuated more than waves that travel along the fiber direction. This is generally known as material anisotropy and is referred to here as diagonal attenuation. Compensation for this effect is described in detail for Targets C-1 and C-2.

Conclusions

The results of the hypervelocity impact test on multi-layer Targets A-1, B-1, and A-2 are as follows:

- Ultrasonic Sensors were successfully bonded to fiberglass Targets A-1, B-1, and A-2 with a Lord 202 Acrylic Adhesive.
- Ultrasonic Sensors operated well in near-vacuum (6-8 Torr) inside the vacuum chamber at Johnson Space Center's White Sands Testing Facility.²
- Impacts created detectable ultrasonic signals at high (>50 kHz) frequencies which should be above flight noise.³

² B1025 sensors also functioned well in deep vacuum of ESEM. Michael Horn, NASA LaRC, email 2005.

- Ultrasonic signals were detected with small, lightweight sensors capable of space flight.⁴⁵
- Wave propagation characteristics of the cross-ply fiberglass target were measured and used in the analysis of the wave signal energy.
- Wave signal energy correlated well with kinetic energy and impact damage.

This test successfully demonstrated the ability for a wing leading edge impact detection system (WLEIDS) to model the kinetic energy response and material damage below, at and above complete penetration of the projectile through the target.

Appendix

The appendices contain the information for each shot and the waveforms. For completeness, and, for usefulness when judging the energy versus damage plots shown in the discussion section above, tables are given at the end that summarize and group together the data for the key test variables.

³ Based on measurement of noise spectra on F16 bulkhead at full throttle, there will not be significant noise power above 50kHz.

⁴ Sensors passed 18,000 g shock test. Henry Whitesel, Naval Surface Warfare Center, verbal communication 1998.

⁵ DWC sensors survived intense radiation environment. Dane Spearing, LANL, verbal communication 2003.

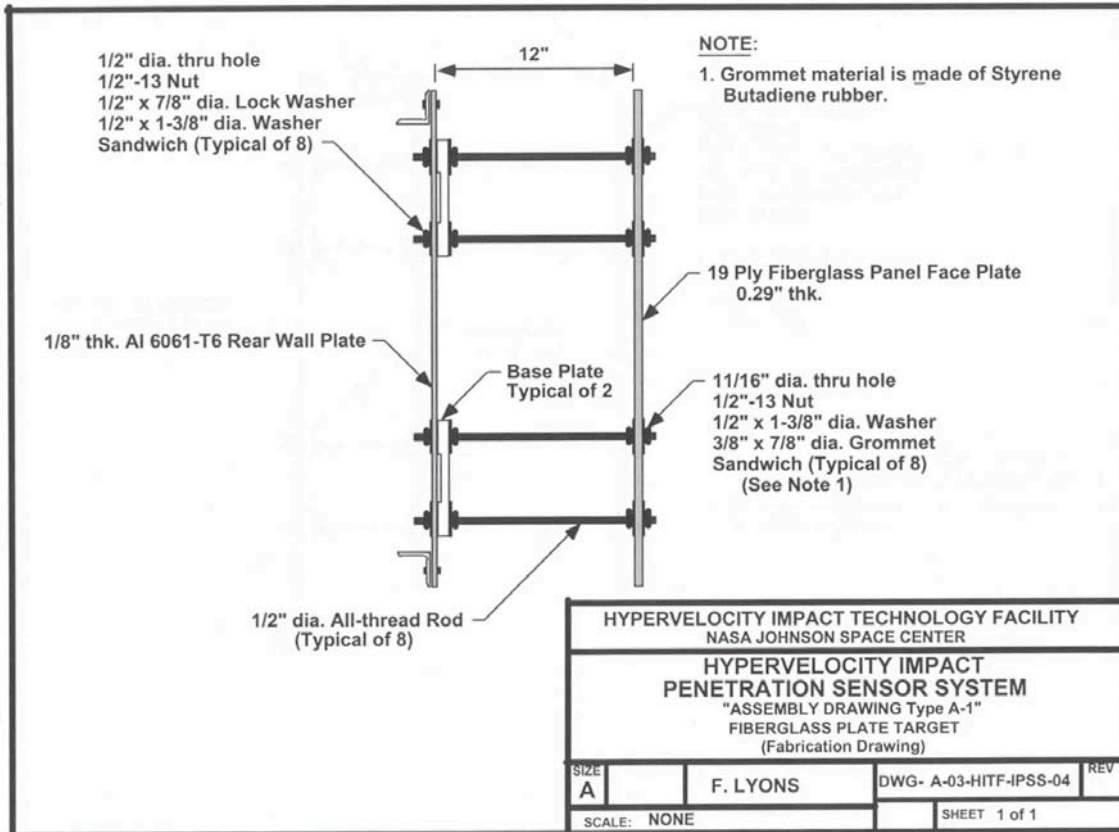


Figure 32: Target A-1 Drawing

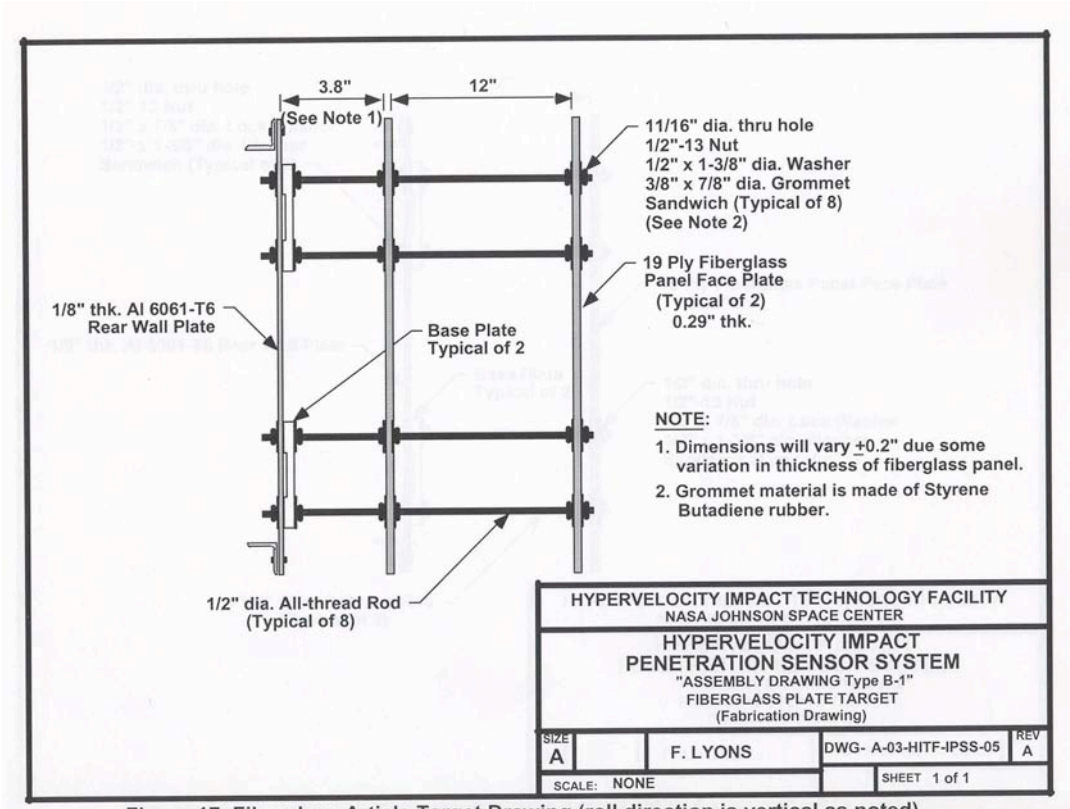


Figure 33: Target B-1 Drawing

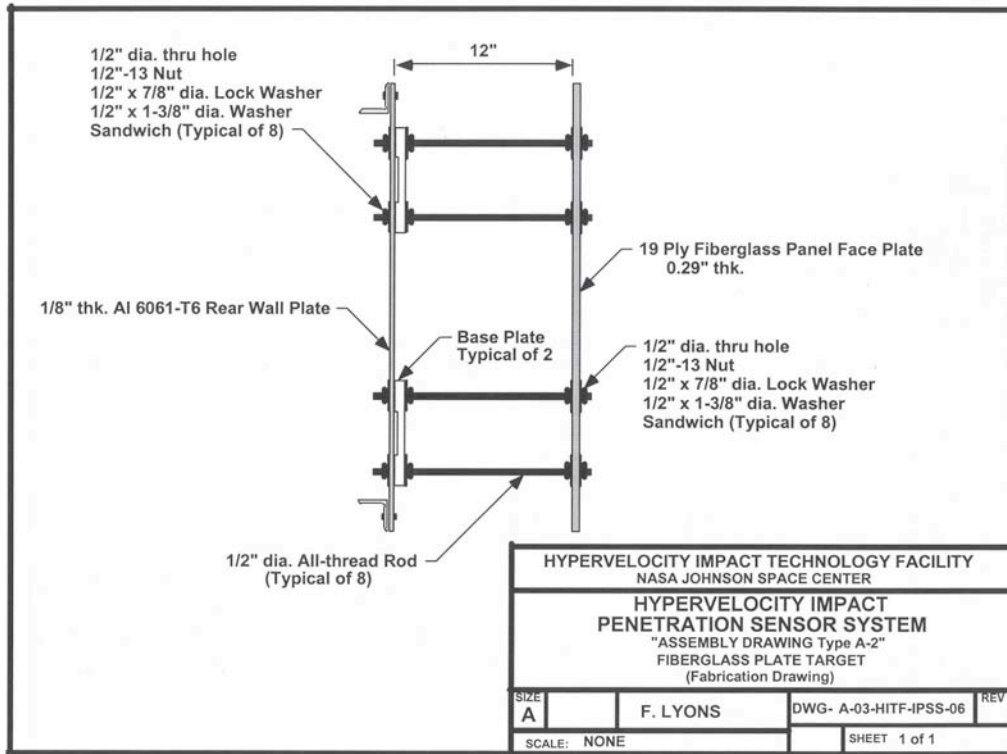


Figure 34: Target A-2 Drawing

Test Conditions Data Sheets

Test conditions for AE (ultrasonic) data acquisition during hypervelocity impact testing

Test date: 11-13-03

Specimen description: 30X30X1 in. Fiberglass target with Aluminum 2nd layer
 Target A-1
 Shot # 1

Impact conditions:

Projectile material and diameter: 1 mm diameter aluminum
 Planned impact coordinates (in.): 12, 20
 Actual impact coordinates (in.): 12.6, 20.7
 AE estimated impact coordinates (in.):
 Planned impact velocity (km/s): 6.8
 Actual impact velocity (km/s): 6.71
 Impact angle: 0

Sensor information:

Ch. #	Sensor Model	x coord. (in.)	Y coord. (in.)	Attenuation at sensor * (dB)	Preamp gain/attenuation (dB)	System gain (dB)	Total gain/attenuation (dB)
1	225	8	5 (Al)	0	-20	0	-20
2	225	22	5 (Al)	0	-20	0	-20
3	225	8	25 (Al)	0	-20	0	-20
4	225	22	25 (Al)	0	-20	0	-20
5	225	6	7 (FG)	-50	0	0	-50
6	225	25	15 (FG)	-50	0	0	-50

- 20 Preliminary estimate for attenuation at sensor based on field measurements. Attenuators calibrated for 50 ohm input, but used for high impedance preamp input. Further laboratory characterization required.

Signal filter settings: 20kHz – 1500 kHz bandpass on all channels

Instrumentation settings:

5 MHz sampling rate
 32k points
 4096 pretrigger points

Comments: Too much attenuation, especially on Ch. 5-6. Channel 5 shows very small signal that is suspect. Problem later traced to bad preamp input connector. EMI type signals seen on all channels at trigger time (819 microseconds) and again later at 1296 microseconds

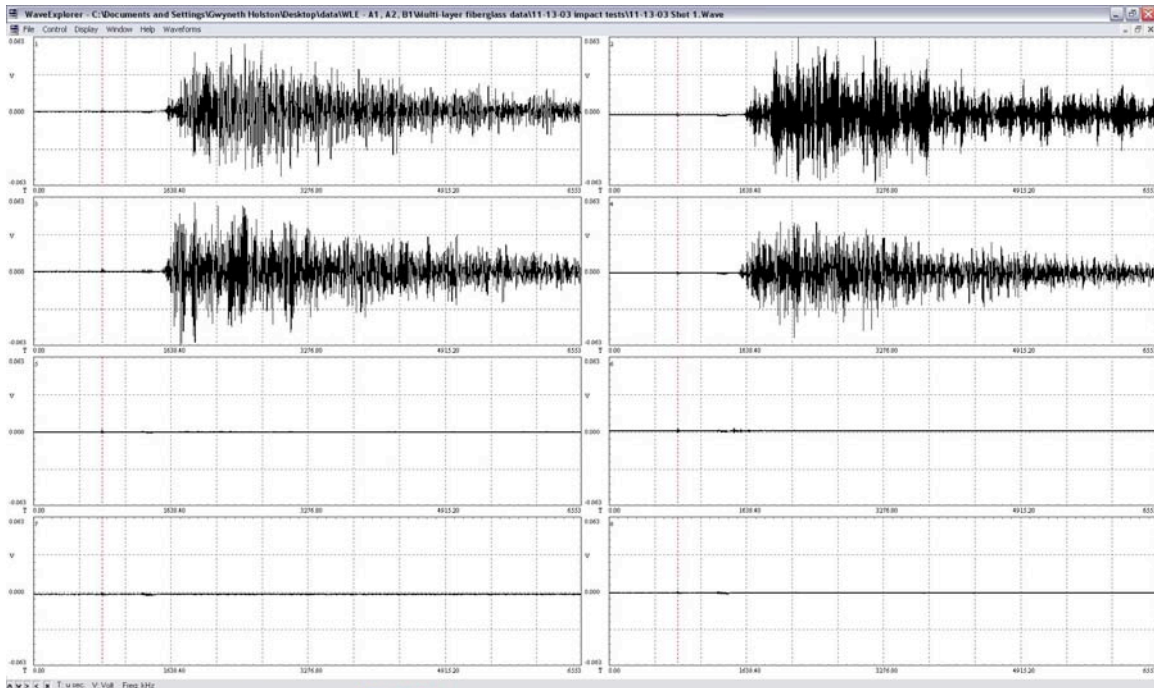


Figure 35: A-1 Shot #1 Impact Waveform

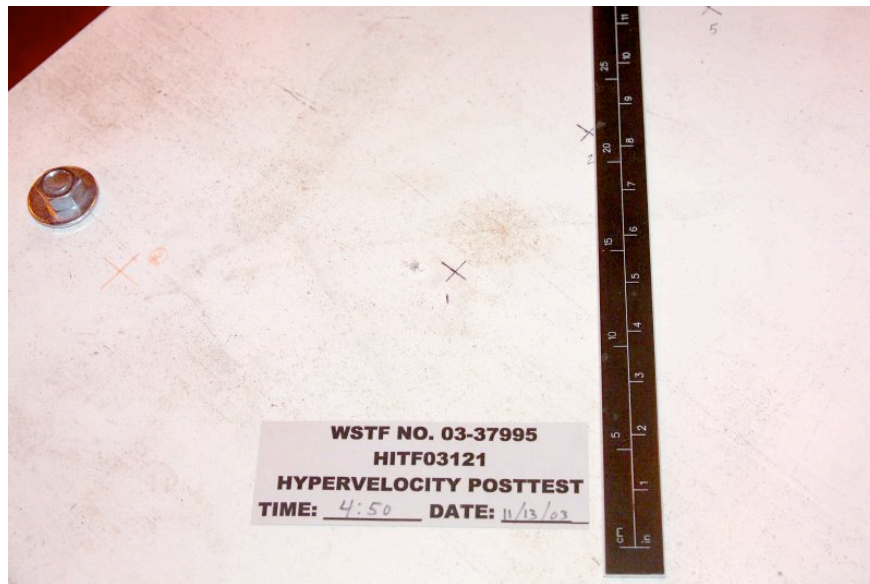


Figure 36: A-1 Shot #1 Impact Damage

Test conditions for AE (ultrasonic) data acquisition during hypervelocity impact testing

Test date: 11-14-03

Specimen description: 30X30X1 in. Fiberglass target with Aluminum 2nd layer
Target A-1
Shot # 2

Impact conditions:

Projectile material and diameter: 1.4 mm diameter aluminum
Planned impact coordinates (in.): 16, 20
Actual impact coordinates (in.): 16.1, 20.1
AE estimated impact coordinates (in.):
Planned impact velocity (km/s): 6.8
Actual impact velocity (km/s): 6.72
Impact angle: 0

Sensor information:

Ch. #	Sensor Model	x coord. (in.)	Y coord. (in.)	Attenuation at sensor * (dB)	Preamp gain/attenuation (dB)	System gain (dB)	Total gain/attenuation (dB)
1	225	8	5 (Al)	0	0	6	6
2	225	22	5 (Al)	0	0	6	6
3	225	8	25 (Al)	0	0	6	6
4	225	22	25 (Al)	0	0	6	6
5	225	6	7 (FG)	-50	0	9	-41
6	225	25	15 (FG)	-50	0	9	-41

20 Preliminary estimate for attenuation at sensor based on field measurements.
Attenuators calibrated for 50 ohm input, but used for high impedance preamp input. Further laboratory characterization required.

Signal filter settings: 20kHz – 1500 kHz bandpass on all channels

Instrumentation settings:

5 MHz sampling rate
32k points
4096 pretrigger points

Comments: All signals in range. Channel 5 acquired on this shot.

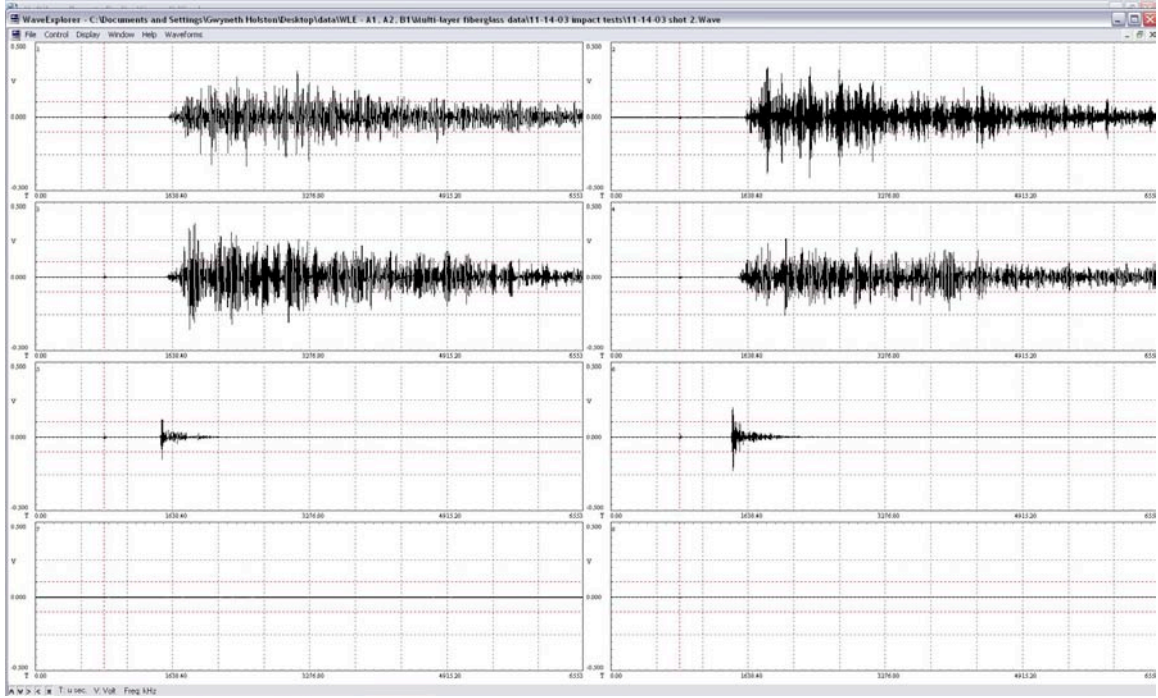


Figure 37: A-1 Shot #2 Impact Waveform

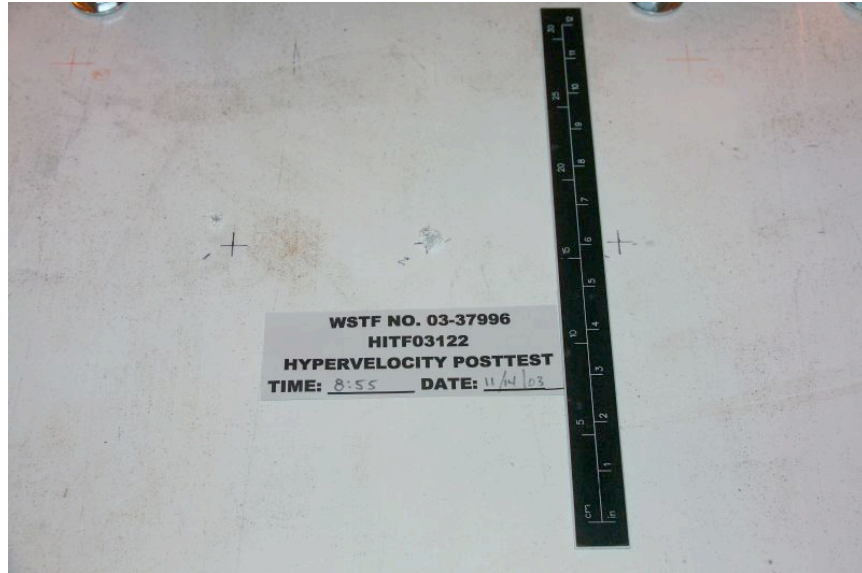


Figure 38: A-1 Shot #2 Impact Damage

Test conditions for AE (ultrasonic) data acquisition during hypervelocity impact testing

Test date: 11-14-03

Specimen description: 30X30X1 in. Fiberglass target with Aluminum 2nd layer
Target A-1
Shot # 3

Impact conditions:

Projectile material and diameter: 1.6 mm diameter aluminum
Planned impact coordinates (in.): 20, 10
Actual impact coordinates (in.): 20.2, 9.75
AE estimated impact coordinates (in.):
Planned impact velocity (km/s): 6.8
Actual impact velocity (km/s): 6.67
Impact angle: 0

Sensor information:

Ch. #	Sensor Model	x coord. (in.)	Y coord. (in.)	Attenuation at sensor * (dB)	Preamp gain/attenuation (dB)	System gain (dB)	Total gain/attenuation (dB)
1	225	8	5 (Al)	0	0	0	0
2	225	22	5 (Al)	0	0	0	0
3	225	8	25 (Al)	0	0	0	0
4	225	22	25 (Al)	0	0	0	0
5	225	6	7 (FG)	-50	0	0	-50
6	225	25	15 (FG)	-50	0	0	-50

20 Preliminary estimate for attenuation at sensor based on field measurements.
Attenuators calibrated for 50 ohm input, but used for high impedance preamp input. Further laboratory characterization required.

Signal filter settings: 20kHz – 1500 kHz bandpass on all channels

Instrumentation settings:

5 MHz sampling rate
32k points
4096 pretrigger points

Comments: All signals in range except some saturation on channel 2. Channel 5 data not acquired because of problem later found to be bad input connector on preamp.

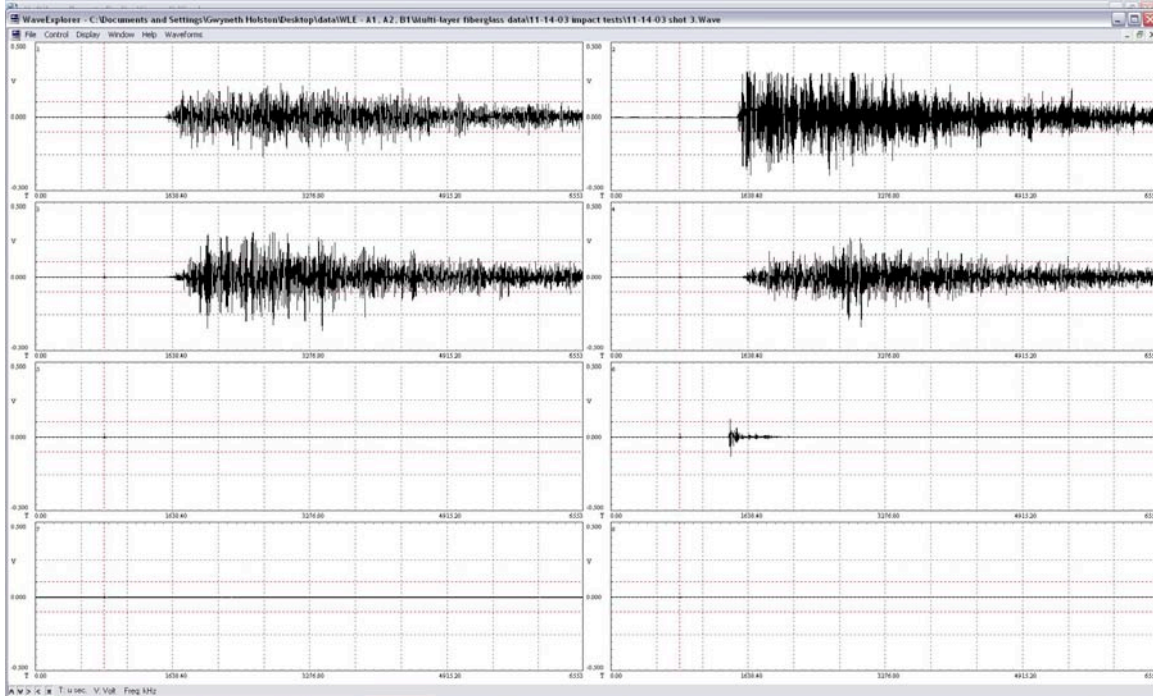


Figure 39: A-1 Shot #3 Impact Waveform

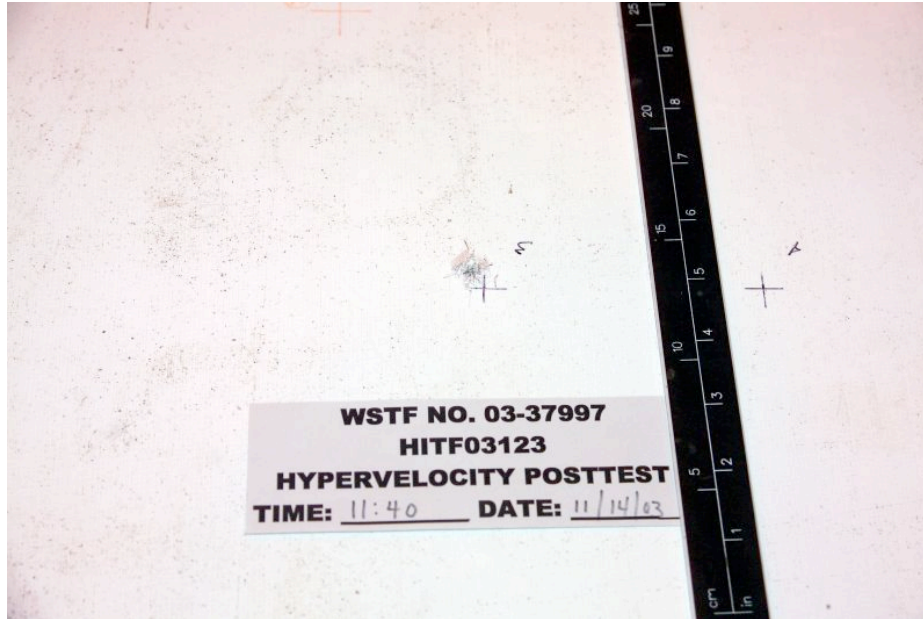


Figure 40: A-1 Shot #3 Impact Damage

Test conditions for AE (ultrasonic) data acquisition during hypervelocity impact testing

Test date: 11-15-03

Specimen description: 30X30X1 in. Fiberglass target with Aluminum 2nd layer
Target A-1
Shot # 5

Impact conditions:

Projectile material and diameter: 5.6 mm diameter aluminum
Planned impact coordinates (in.): 20, 17
Actual impact coordinates (in.): 20.2, 17.1
AE estimated impact coordinates (in.):
Planned impact velocity (km/s): 6.8
Actual impact velocity (km/s): 6.86
Impact angle: 0

Sensor information:

Ch. #	Sensor Model	x coord. (in.)	Y coord. (in.)	Attenuation at sensor * (dB)	Preamp gain/attenuation (dB)	System gain (dB)	Total gain/attenuation (dB)
1	225	8	5 (Al)	0	0	36	36
2	225	22	5 (Al)	0	0	36	36
3	225	8	25 (Al)	0	0	36	36
4	225	22	25 (Al)	0	0	36	36
5	225	6	7 (FG)	-50	-20	33	-37
6	225	25	15 (FG)	-50	-20	33	-37

20 Preliminary estimate for attenuation at sensor based on field measurements. Attenuators calibrated for 50 ohm input, but used for high impedance preamp input. Further laboratory characterization required.

Signal filter settings: 20kHz – 1500 kHz bandpass on all channels

Instrumentation settings:

5 MHz sampling rate
32k points
4096 pretrigger points

Comments: Gain improperly set much too high on Channels 1-4 causing much saturation. Signals obtained and in range on Ch. 5-6. Large EMI signals observed on all channels at and just after trigger. Sensors 2 and 6 were knocked off of the specimen and had to be rebounded before the next test.

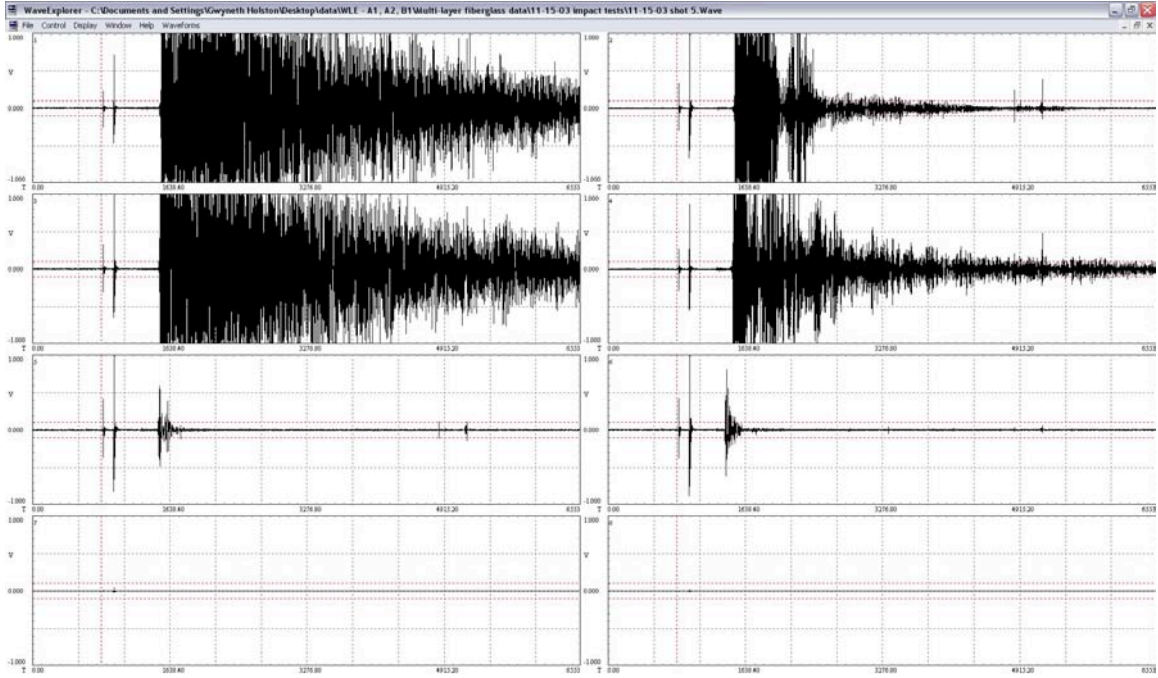


Figure 41: A-1 Shot #5 Impact Waveform

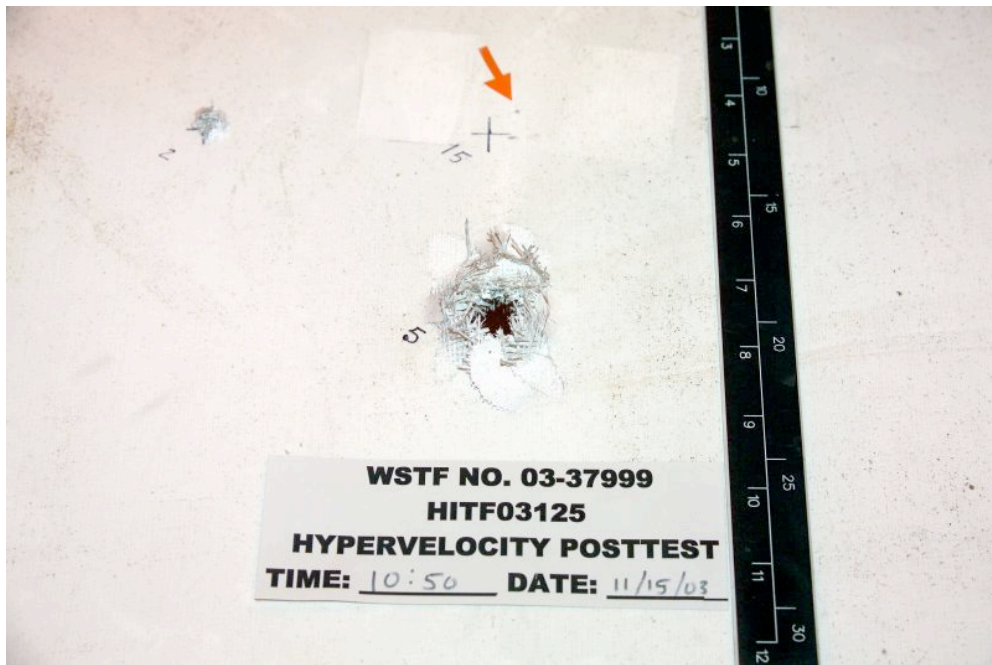


Figure 42: A-1 Shot #5 Impact Damage

Test conditions for AE (ultrasonic) data acquisition during hypervelocity impact testing

Test date: 11-15-03

Specimen description: 30X30X1 in. Fiberglass target with Aluminum 2nd layer
Target A-1
Shot # 6

Impact conditions:

Projectile material and diameter: 6.0 mm diameter aluminum
Planned impact coordinates (in.): 12, 10
Actual impact coordinates (in.): 11.9, 9.75
AE estimated impact coordinates (in.):
Planned impact velocity (km/s): 6.8
Actual impact velocity (km/s): 6.82
Impact angle: 0

Sensor information:

Ch. #	Sensor Model	x coord. (in.)	Y coord. (in.)	Attenuation at sensor * (dB)	Preamp gain/attenuation (dB)	System gain (dB)	Total gain/attenuation (dB)
1	225	8	5 (Al)	0	0	12	12
2	225	22	5 (Al)	0	0	12	12
3	225	8	25 (Al)	0	0	12	12
4	225	22	25 (Al)	0	0	12	12
5	225	6	7 (FG)	-50	-20	12	-58
6	225	25	15 (FG)	-50	-20	12	-58

20 Preliminary estimate for attenuation at sensor based on field measurements. Attenuators calibrated for 50 ohm input, but used for high impedance preamp input. Further laboratory characterization required.

Signal filter settings: 20kHz – 1500 kHz bandpass on all channels

Instrumentation settings:

5 MHz sampling rate
32k points
4096 pretrigger points

Comments: Signals in range although very small on Ch. 5-6. Sensor 1 was knocked off specimen during impact. A much shortened time signal is usually observed when the sensor comes off the target.

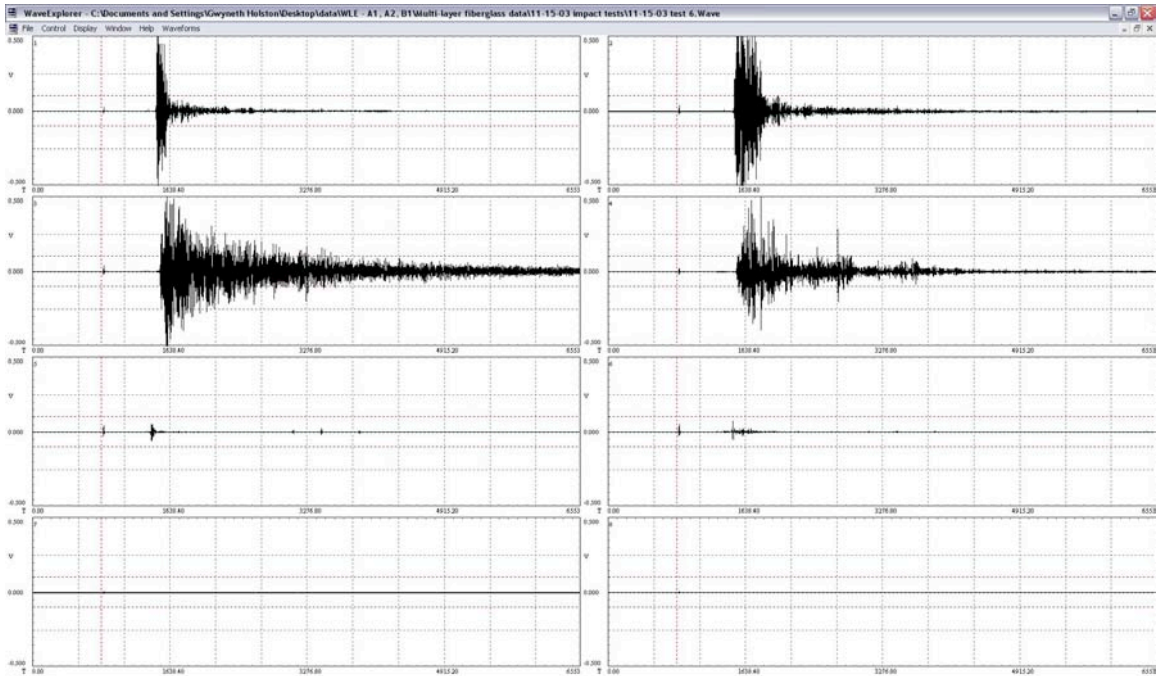


Figure 43: A-1 Shot #6 Impact Waveform

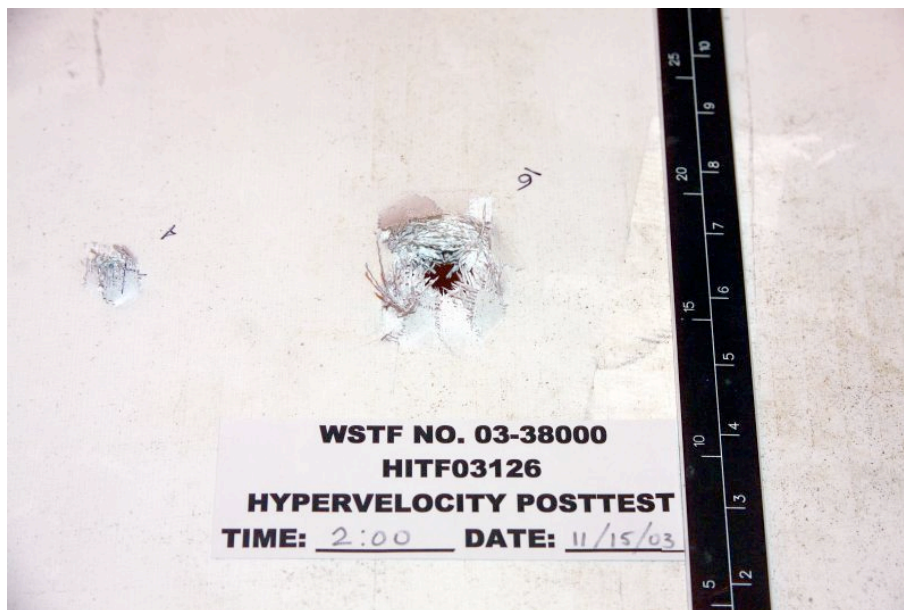


Figure 44: A-1 Shot #6 Impact Damage

Test conditions for AE (ultrasonic) data acquisition during hypervelocity impact testing

Test date: 11-17-03

Specimen description: 30X30X1 in. Fiberglass target with Fiberglass 2nd layer and
Aluminum 3rd layer
Target B-1
Shot # 7

Impact conditions:

Projectile material and diameter: 1.6 mm diameter aluminum
Planned impact coordinates (in.): 12, 20
Actual impact coordinates (in.): 11.8, 19.6
AE estimated impact coordinates (in.):
Planned impact velocity (km/s): 6.8
Actual impact velocity (km/s): 6.82
Impact angle: 0

Sensor information:

Ch. #	Sensor Model	x coord. (in.)	Y coord. (in.)	Attenuation at sensor * (dB)	Preamp gain/attenuation (dB)	System gain (dB)	Total gain/attenuation (dB)
1	225	8	5 (FG 2)	0	0	6	6
2	225	22	5 (FG 2)	0	0	6	6
3	225	8	25 (FG 2)	0	0	6	6
4	225	22	25 (FG 2)	0	0	6	6
5	225	6	7 (FG)	-50	-20	6	-64
6	225	25	15 (FG)	-50	-20	6	-64
7	225	6	7 (Al)	0	0	3	3
8	225	25	15 (Al)	0	0	3	3

20 Preliminary estimate for attenuation at sensor based on field measurements. Attenuators calibrated for 50 ohm input, but used for high impedance preamp input. Further laboratory characterization required.

Signal filter settings: 20kHz – 1500 kHz bandpass on all channels

Instrumentation settings:

5 MHz sampling rate
32k points
4096 pretrigger points

Comments: Signals in range on all channels and channel 5 signal acquired. EMI near trigger much smaller.

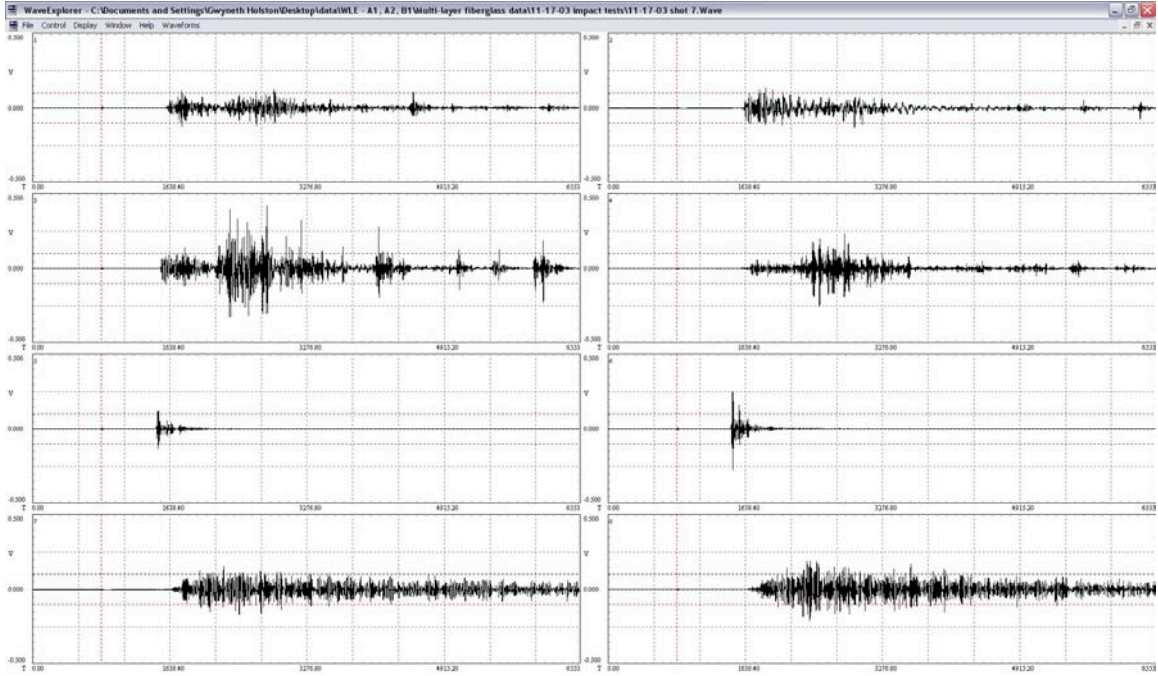


Figure 45: B-1 Shot #7 Impact Waveform

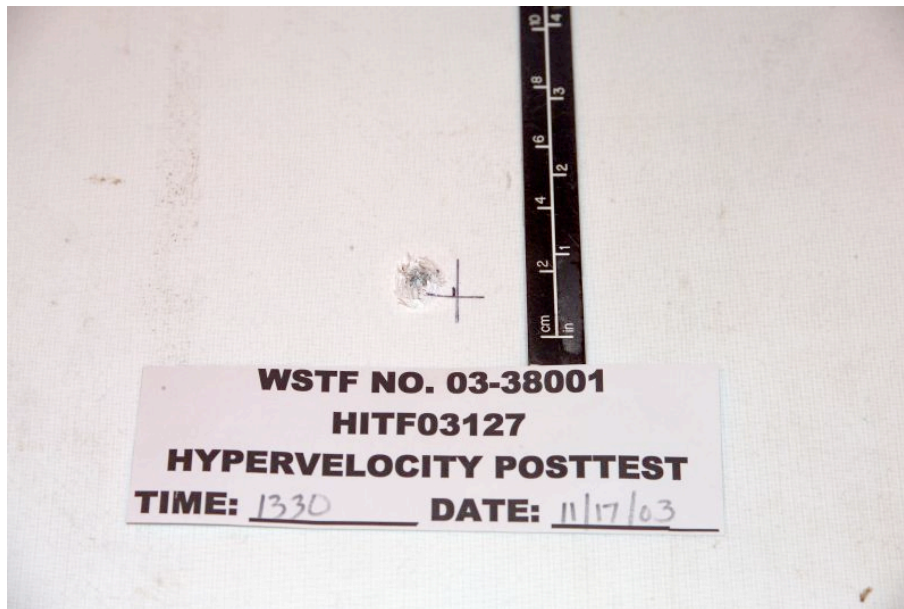


Figure 46: B-1 Shot #7 Impact Waveform

Test conditions for AE (ultrasonic) data acquisition during hypervelocity impact testing

Test date: 11-17-03

Specimen description: 30X30X1 in. Fiberglass target with Fiberglass 2nd layer and
Aluminum 3rd layer
Target B-1
Shot # 8

Impact conditions:

Projectile material and diameter: 2 mm diameter aluminum
Planned impact coordinates (in.): 12, 10
Actual impact coordinates (in.): 11.9, 9.6
AE estimated impact coordinates (in.):
Planned impact velocity (km/s): 6.8
Actual impact velocity (km/s): 6.75
Impact angle: 0

Sensor information:

Ch. #	Sensor Model	x coord. (in.)	Y coord. (in.)	Attenuation at sensor * (dB)	Preamp gain/attenuation (dB)	System gain (dB)	Total gain/attenuation (dB)
1	225	8	5 (FG 2)	0	-20	12	-8
2	225	22	5 (FG 2)	0	-20	12	-8
3	225	8	25 (FG 2)	0	-20	12	-8
4	225	22	25 (FG 2)	0	-20	12	-8
5	225	6	7 (FG)	-50	-20	12	-58
6	225	25	15 (FG)	-50	-20	12	-58
7	225	6	7 (Al)	0	-20	12	-8
8	225	25	15 (Al)	0	-20	12	-8

- 20 Preliminary estimate for attenuation at sensor based on field measurements. Attenuators calibrated for 50 ohm input, but used for high impedance preamp input. Further laboratory characterization required.

Signal filter settings: 20kHz – 1500 kHz bandpass on all channels

Instrumentation settings:

5 MHz sampling rate
32k points
4096 pretrigger points

Comments: Signals in range on all channels although small on channel 6-8. Channel 5 signal not acquired because of problem later found to be bad input connector on preamp.

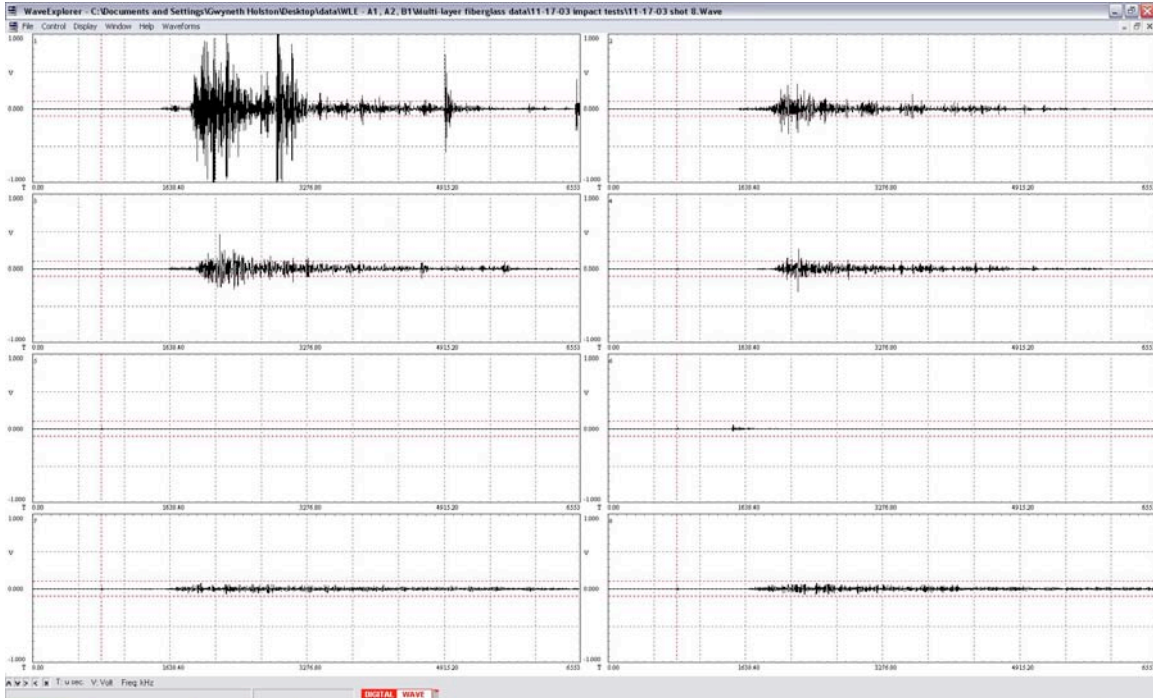


Figure 47: B-1 Shot #8 Impact Waveform

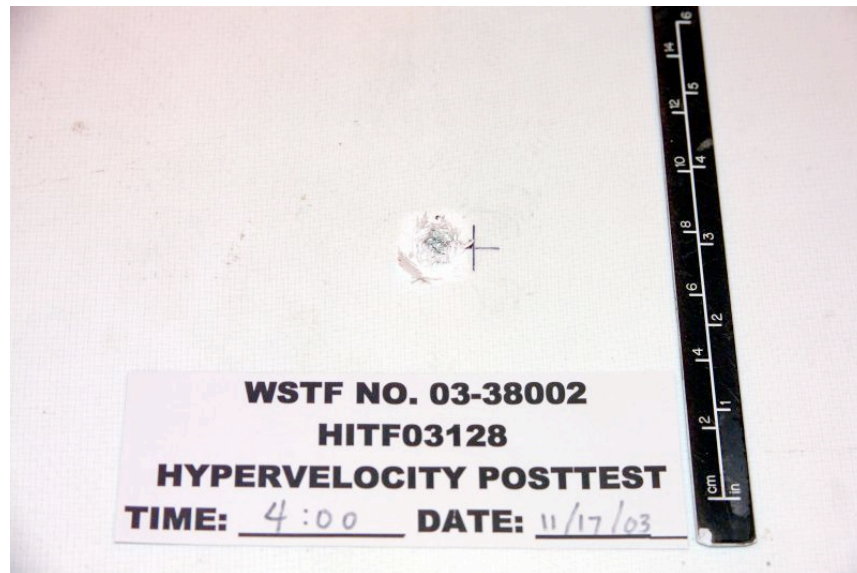


Figure 48: B-1 Shot #8 Impact Damage

Test conditions for AE (ultrasonic) data acquisition during hypervelocity impact testing

Test date: 11-19-03

Specimen description: 30X30X1 in. Fiberglass target with Fiberglass 2nd layer and
Aluminum 3rd layer

Target B-1

Shot # 9

Impact conditions:

Projectile material and diameter: 5.6 mm diameter aluminum

Planned impact coordinates (in.): 18, 20

Actual impact coordinates (in.): 18, 19.2

AE estimated impact coordinates (in.):

Planned impact velocity (km/s): 6.8

Actual impact velocity (km/s): 6.96

Impact angle: 0

Sensor information:

Ch. #	Sensor Model	x coord. (in.)	Y coord. (in.)	Attenuation at sensor * (dB)	Preamp gain/attenuation (dB)	System gain (dB)	Total gain/attenuation (dB)
1	225	8	5 (FG 2)	-50	0	12	-38
2	225	22	5 (FG 2)	-50	0	12	-38
3	225	8	25 (FG 2)	-50	0	12	-38
4	225	22	25 (FG 2)	-50	0	12	-38
5	225	6	7 (FG)	-50	-20	18	-52
6	225	25	15 (FG)	-50	-20	18	-52
7	225	6	7 (Al)	-50	20	12	-18
8	225	25	15 (Al)	-50	20	12	-18

- 20 Preliminary estimate for attenuation at sensor based on field measurements. Attenuators calibrated for 50 ohm input, but used for high impedance preamp input. Further laboratory characterization required.

Signal filter settings: 20kHz – 1500 kHz bandpass on all channels

Instrumentation settings:

5 MHz sampling rate

32k points

4096 pretrigger points

Comments: Saturation on Channel 4 only. Too much attenuation on channels 7-8. EMI signals observed at trigger time. Sensor 6 became disbonded as was evident in signal. Another EMI signal generated when sensor 6 stops functioning. Sensor 6 was tested and replace for next shot.

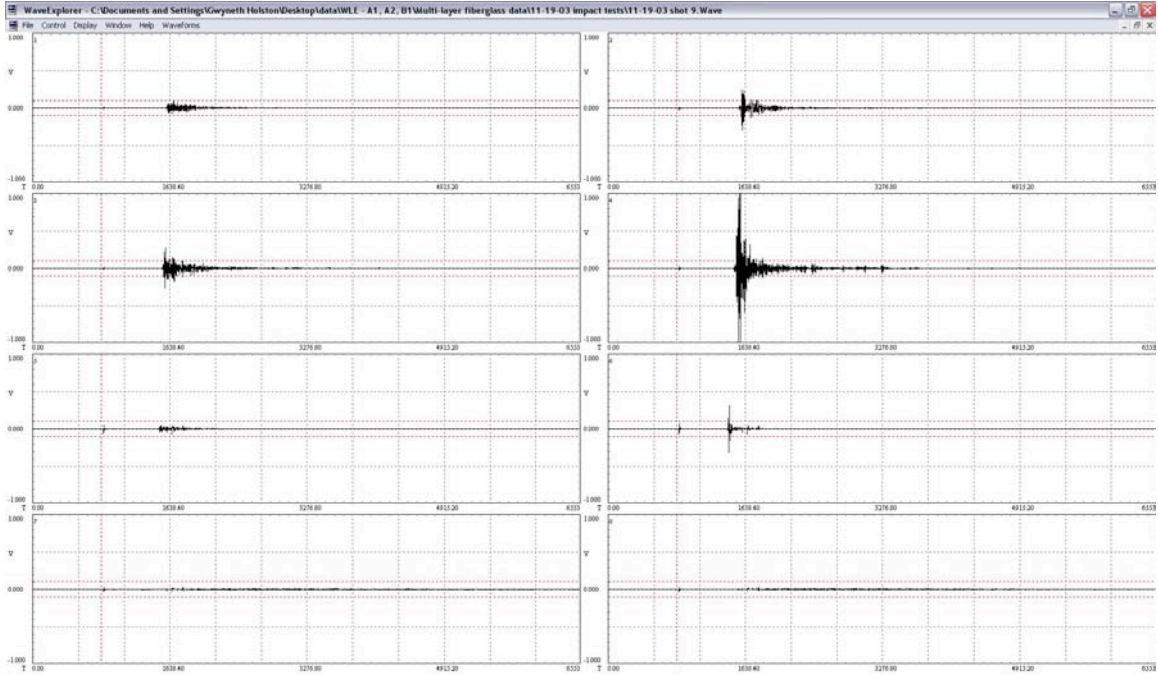


Figure 49: B-1 Shot # 9 Impact Waveform

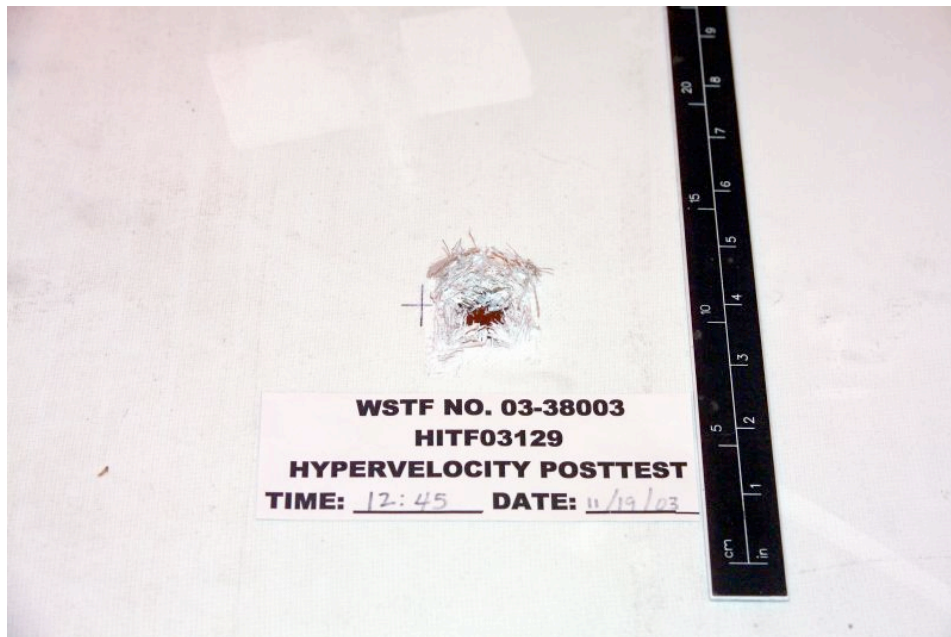


Figure 50: B-1 Shot # 9 Impact Damage

Test conditions for AE (ultrasonic) data acquisition during hypervelocity impact testing

Test date: 11-19-03

Specimen description: 30X30X1 in. Fiberglass target with Fiberglass 2nd layer and
Aluminum 3rd layer

Target B-1

Shot # 10

Impact conditions:

Projectile material and diameter: 6 mm diameter aluminum

Planned impact coordinates (in.): 18, 10

Actual impact coordinates (in.): 17.8, 10.1

AE estimated impact coordinates (in.):

Planned impact velocity (km/s): 6.8

Actual impact velocity (km/s): 6.85

Impact angle: 0

Sensor information:

Ch. #	Sensor Model	x coord. (in.)	Y coord. (in.)	Attenuation at sensor * (dB)	Preamp gain/attenuation (dB)	System gain (dB)	Total gain/attenuation (dB)
1	225	8	5 (FG 2)	-50	-20	18	-52
2	225	22	5 (FG 2)	-50	-20	18	-52
3	225	8	25 (FG 2)	-50	-20	18	-52
4	225	22	25 (FG 2)	-50	-20	18	-52
5	225	6	7 (FG)	-50	-20	12	-58
6	225	25	15 (FG)	-50	-20	12	-58
7	225	6	7 (Al)	0	0	3	3
8	225	25	15 (Al)	0	0	3	3

- 20 Preliminary estimate for attenuation at sensor based on field measurements. Attenuators calibrated for 50 ohm input, but used for high impedance preamp input. Further laboratory characterization required.

Signal filter settings: 20kHz – 1500 kHz bandpass on all channels

Instrumentation settings:

5 MHz sampling rate

32k points

4096 pretrigger points

Comments: Saturation on Channel 7-8. EMI pulses seen at trigger time and also later in signals. No sensors debonded during test.

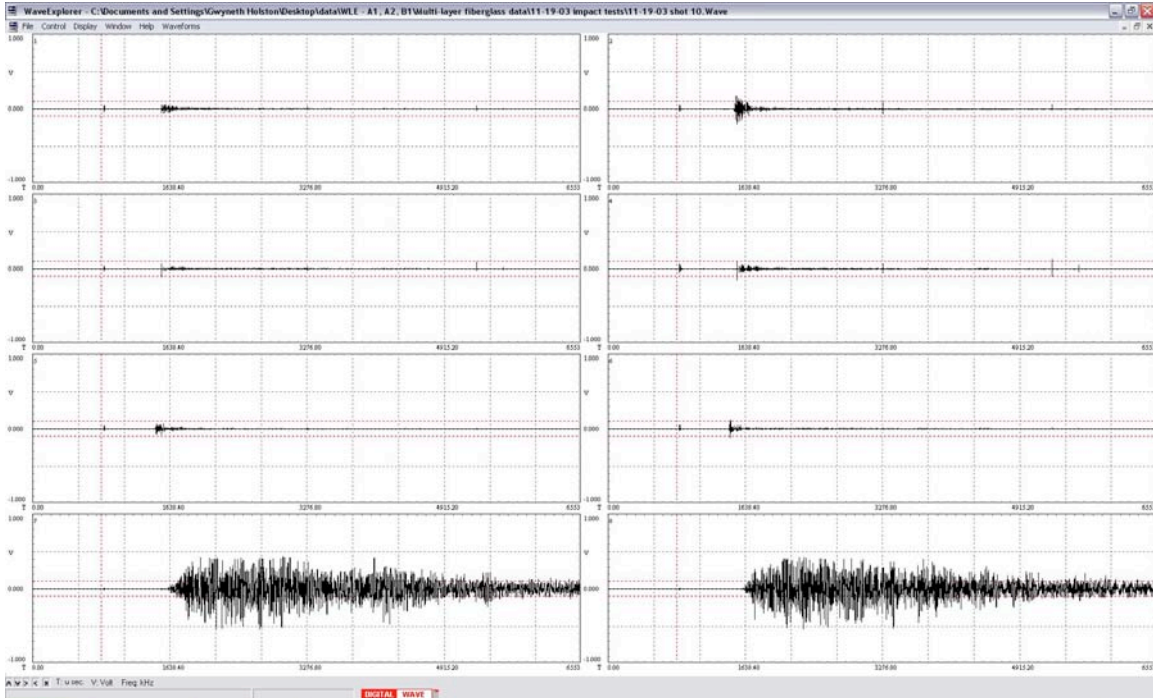


Figure 51: B-1 Shot #10 Impact Waveform

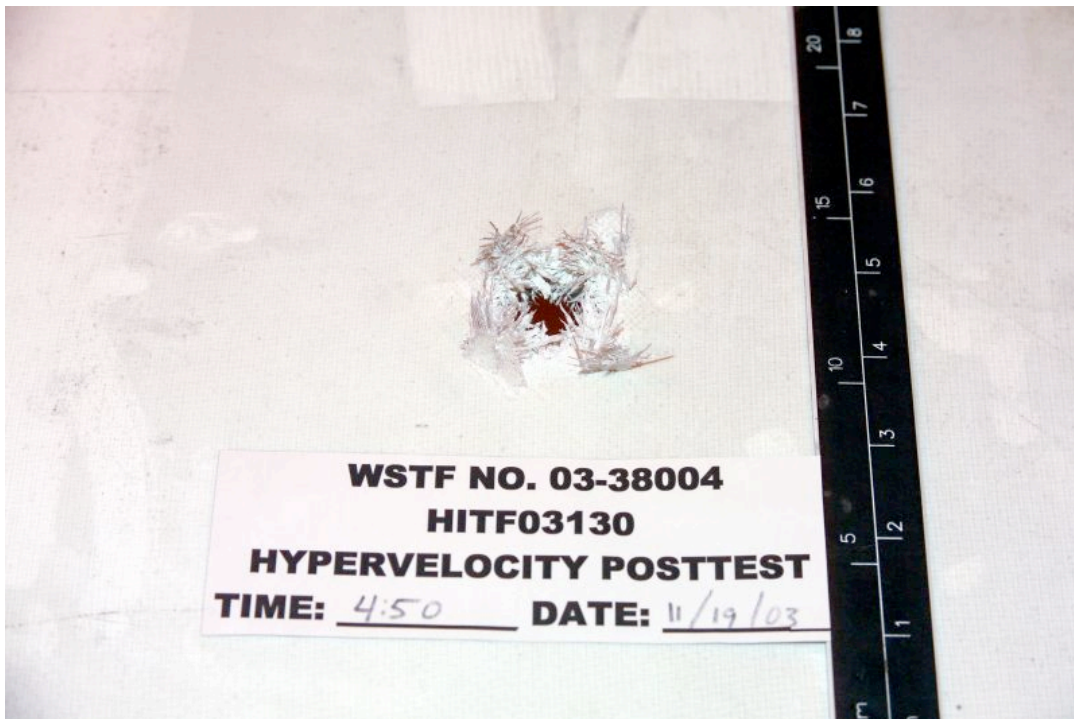


Figure 52: B-1 Shot #10 Impact Damage

Test conditions for AE (ultrasonic) data acquisition during hypervelocity impact testing

Test date: 11-18-03

Specimen description: 30X30X1 in. Fiberglass target with Aluminum 2nd layer
 No grommets around standoff rods
 Target A-2
 Shot # 11

Impact conditions:

Projectile material and diameter: 1 mm diameter aluminum
 Planned impact coordinates (in.): 12, 20
 Actual impact coordinates (in.): 11.8, 19.7
 AE estimated impact coordinates (in.):
 Planned impact velocity (km/s): 6.8
 Actual impact velocity (km/s): 6.72
 Impact angle: 0

Sensor information:

Ch. #	Sensor Model	x coord. (in.)	Y coord. (in.)	Attenuation at sensor * (dB)	Preamp gain/attenuation (dB)	System gain (dB)	Total gain/attenuation (dB)
1	225	8	5 (Al)	0	0	12	12
2	225	22	5 (Al)	0	0	12	12
3	225	8	25 (AL)	0	0	12	12
4	225	22	25 (AL)	0	0	12	12
5	225	6	7 (FG)	-50	0	12	-38
6	225	25	15 (FG)	-50	0	12	-38

- 20 Preliminary estimate for attenuation at sensor based on field measurements. Attenuators calibrated for 50 ohm input, but used for high impedance preamp input. Further laboratory characterization required.

Signal filter settings: 20kHz – 1500 kHz bandpass on all channels

Instrumentation settings:

5 MHz sampling rate
 32k points
 4096 pretrigger points

Comments: Signals saturated on channels 1-3 later in signal, not in direct arrivals. Signal acquired for this impact on channel 5. Channels 1-4 compared to Shot 1 on panel A-1 (with grommets) and showed ~14 dB higher amplitude without grommets. Channel 6 was similar in amplitude to the Shot 1 Channel 6.

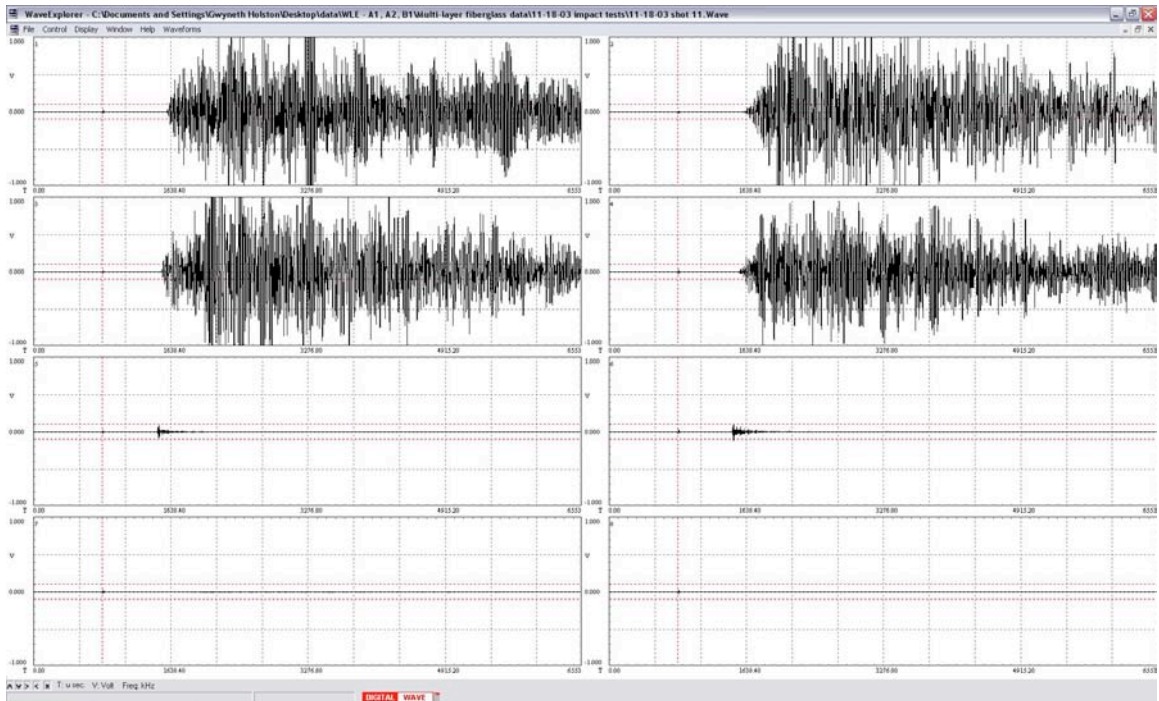


Figure 53: A-2 Shot #11 Impact Waveform

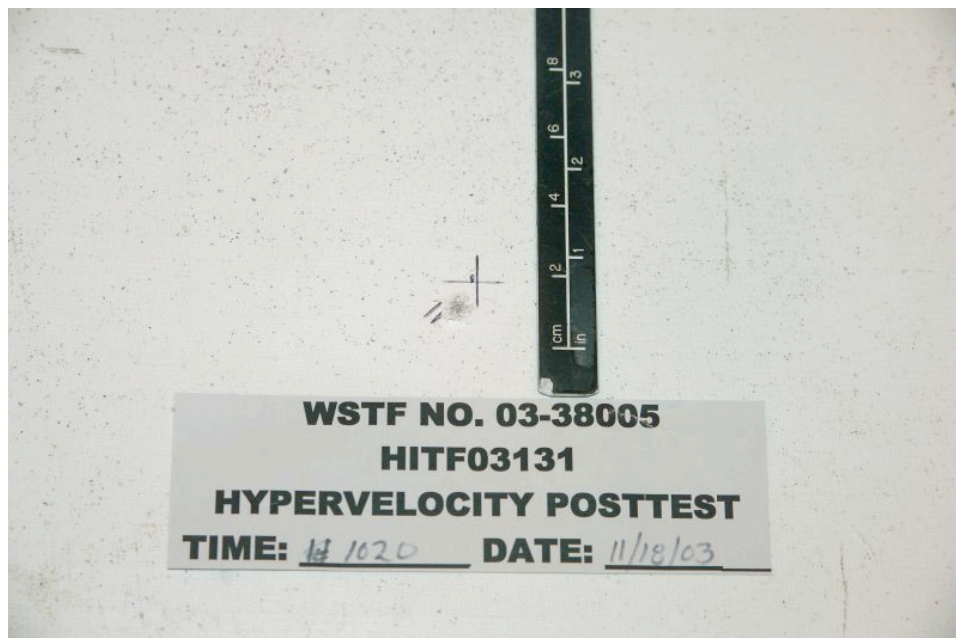


Figure 54: A-2 Shot #11 Impact Damage

Test conditions for AE (ultrasonic) data acquisition during hypervelocity impact testing

Test date: 11-18-03

Specimen description: 30X30X1 in. Fiberglass target with Aluminum 2nd layer
 No grommets around standoff rods
 Target A-2
 Shot # 12

Impact conditions:

Projectile material and diameter: 1.4 mm diameter aluminum
 Planned impact coordinates (in.): 18, 20
 Actual impact coordinates (in.): 17.5, 19.9
 AE estimated impact coordinates (in.):
 Planned impact velocity (km/s): 6.8
 Actual impact velocity (km/s): 6.62
 Impact angle: 0

Sensor information:

Ch. #	Sensor Model	x coord. (in.)	Y coord. (in.)	Attenuation at sensor * (dB)	Preamp gain/attenuation (dB)	System gain (dB)	Total gain/attenuation (dB)
1	225	8	5 (Al)	0	-20	9	9
2	225	22	5 (Al)	0	-20	9	9
3	225	8	25 (AL)	0	-20	9	9
4	225	22	25 (AL)	0	-20	9	9
5	225	6	7 (FG)	-50	0	9	-41
6	225	25	15 (FG)	-50	0	9	-41

- 20 Preliminary estimate for attenuation at sensor based on field measurements. Attenuators calibrated for 50 ohm input, but used for high impedance preamp input. Further laboratory characterization required.

Signal filter settings: 20kHz – 1500 kHz bandpass on all channels

Instrumentation settings:

5 MHz sampling rate
 32k points
 4096 pretrigger points

Comments: All signals in range. Channel 5 not recorded because of problem later identified as bad input connector on preamp. Channels 1-4 compared to Shot 2 on panel A-1 (with grommets) and showed ~14 dB higher amplitude without grommets. Channel 6 was similar in amplitude to the Shot 1 Channel 6.

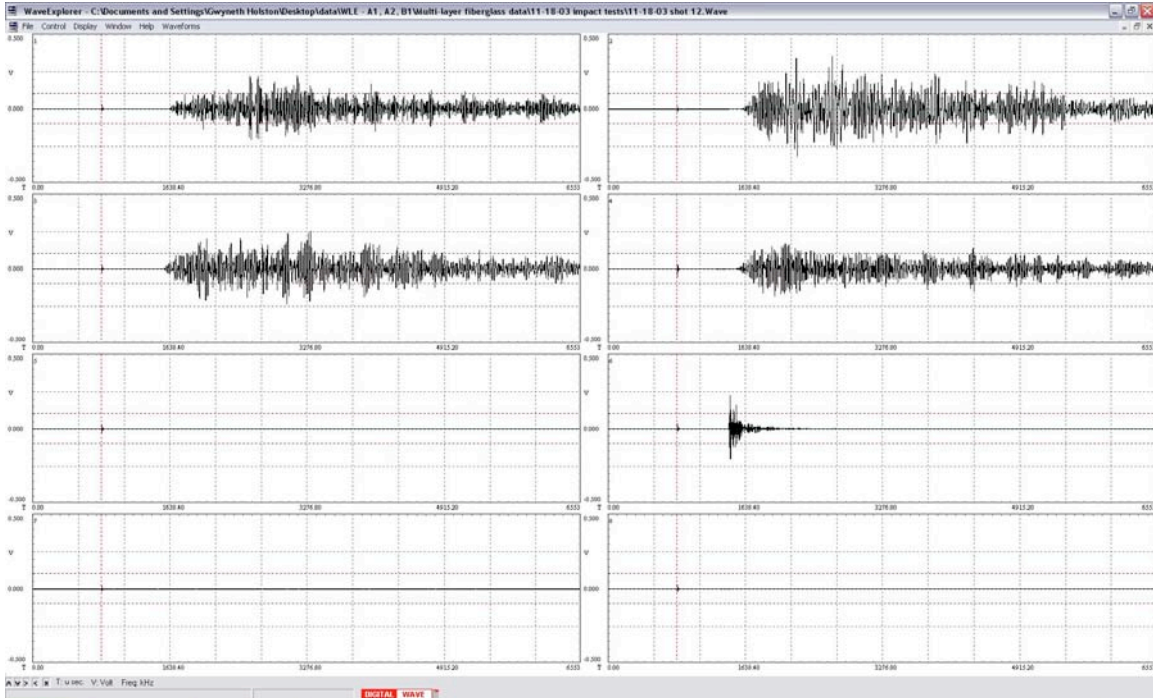


Figure 55: A-2 Shot #12 Impact Waveform

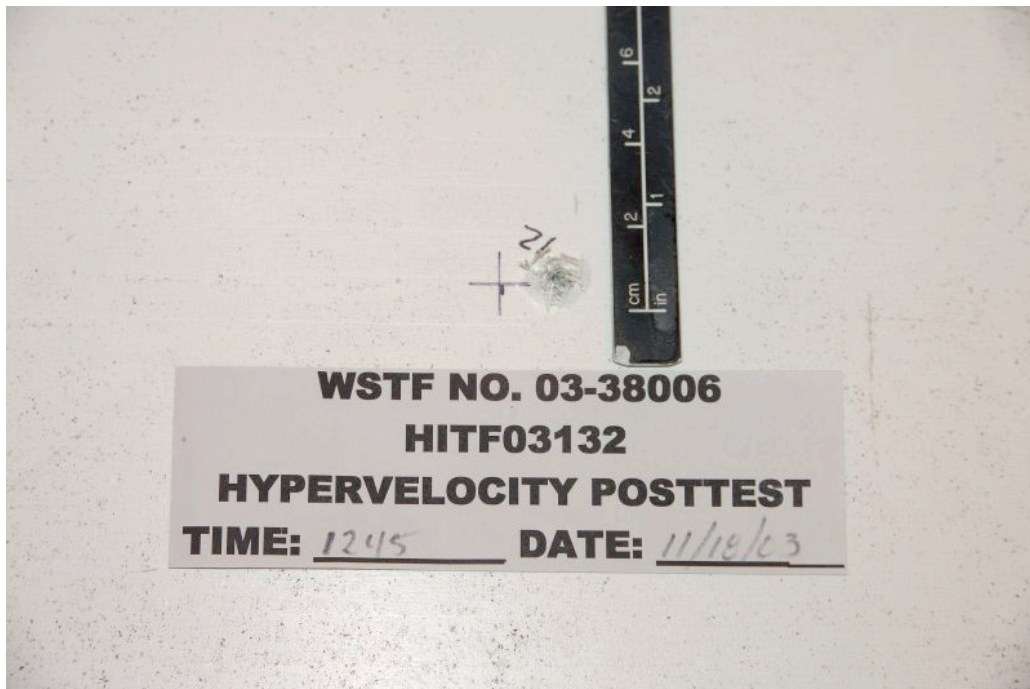


Figure 56: A-2 Shot #12 Impact Damage

Test conditions for AE (ultrasonic) data acquisition during hypervelocity impact testing

Test date: 11-18-03

Specimen description: 30X30X1 in. Fiberglass target with Aluminum 2nd layer
 No grommets around standoff rods
 Target A-2
 Shot # 13

Impact conditions:

Projectile material and diameter: 1.6 mm diameter aluminum
 Planned impact coordinates (in.): 12, 10
 Actual impact coordinates (in.): 12.3, 10.1
 AE estimated impact coordinates (in.):
 Planned impact velocity (km/s): 6.8
 Actual impact velocity (km/s): 6.69
 Impact angle: 0

Sensor information:

Ch. #	Sensor Model	x coord. (in.)	Y coord. (in.)	Attenuation at sensor * (dB)	Preamp gain/attenuation (dB)	System gain (dB)	Total gain/attenuation (dB)
1	225	8	5 (Al)	0	-20	3	-17
2	225	22	5 (Al)	0	-20	3	-17
3	225	8	25 (AL)	0	-20	3	-17
4	225	22	25 (AL)	0	-20	3	-17
5	225	6	7 (FG)	-50	0	3	-47
6	225	25	15 (FG)	-50	0	3	-47

20 Preliminary estimate for attenuation at sensor based on field measurements. Attenuators calibrated for 50 ohm input, but used for high impedance preamp input. Further laboratory characterization required.

Signal filter settings: 20kHz – 1500 kHz bandpass on all channels

Instrumentation settings:

5 MHz sampling rate
 32k points
 4096 pretrigger points

Comments: All signals in range. Preamp was replace on ch. 5 eliminating problem that caused previous loss of data on this channel. Again, signals on ch 1-4 compared to shot 3 on panel A-1 (w/grommets) and similar ~14 dB signal change observed.

Test conditions for AE (ultrasonic) data acquisition during hypervelocity impact testing

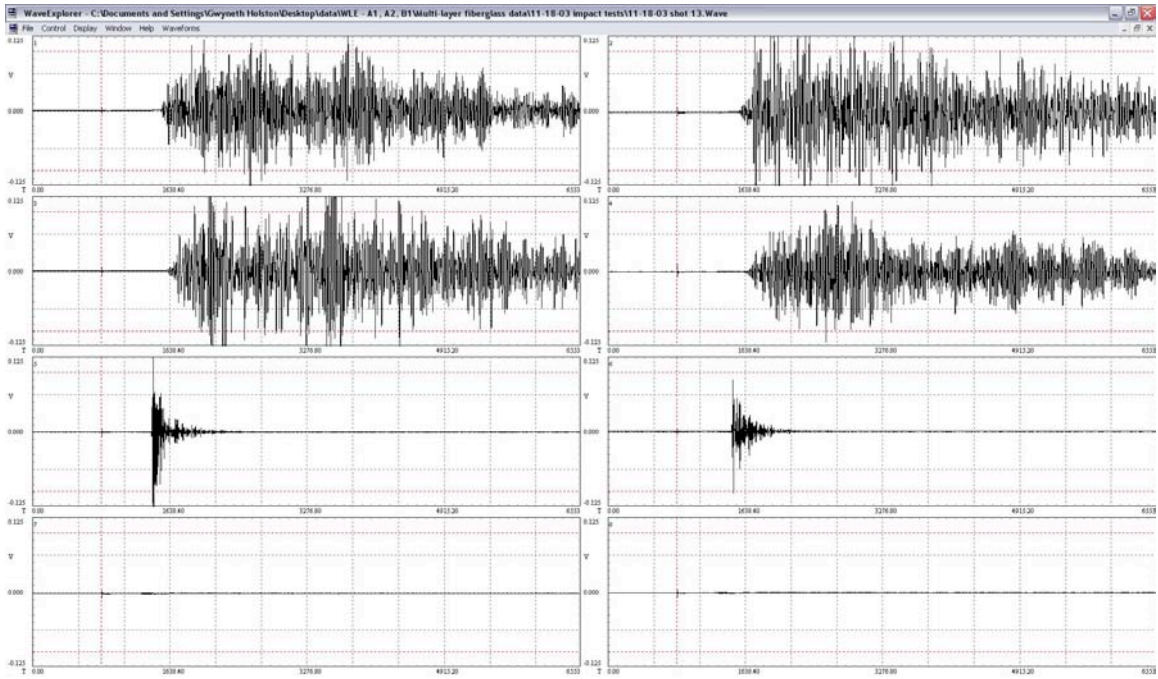


Figure 57: A-2 Shot #13 Impact Waveform

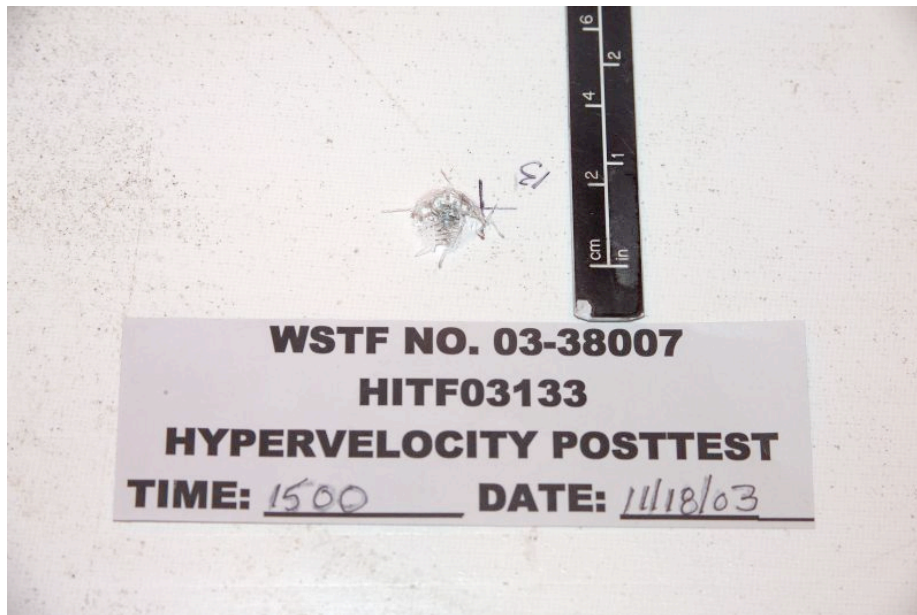


Figure 58: A-2 Shot #13 Impact Damage

Test date: 11-18-03

Specimen description: 30X30X1 in. Fiberglass target with Aluminum 2nd layer
 No grommets around standoff rods
 Target A-2
 Shot # 14

Impact conditions:

Projectile material and diameter: 2 mm diameter aluminum
 Planned impact coordinates (in.): 18, 10
 Actual impact coordinates (in.): 18.6, 10.1
 AE estimated impact coordinates (in.):
 Planned impact velocity (km/s): 6.8
 Actual impact velocity (km/s): 6.75
 Impact angle: 0

Sensor information:

Ch. #	Sensor Model	x coord. (in.)	Y coord. (in.)	Attenuation at sensor * (dB)	Preamp gain/attenuation (dB)	System gain (dB)	Total gain/attenuation (dB)
1	225	8	5 (Al)	0	-20	3	-17
2	225	22	5 (Al)	0	-20	3	-17
3	225	8	25 (AL)	0	-20	3	-17
4	225	22	25 (AL)	0	-20	3	-17
5	225	6	7 (FG)	-50	0	3	-47
6	225	25	15 (FG)	-50	0	3	-47

20 Preliminary estimate for attenuation at sensor based on field measurements.
 Attenuators calibrated for 50 ohm input, but used for high impedance preamp input. Further laboratory characterization required.

Signal filter settings: 20kHz – 1500 kHz bandpass on all channels

Instrumentation settings:

5 MHz sampling rate
 32k points
 4096 pretrigger points

Comments: Again all signals in range. No comparison with signal from shot 4 possible as shot 4 data was lost because of a computer error.

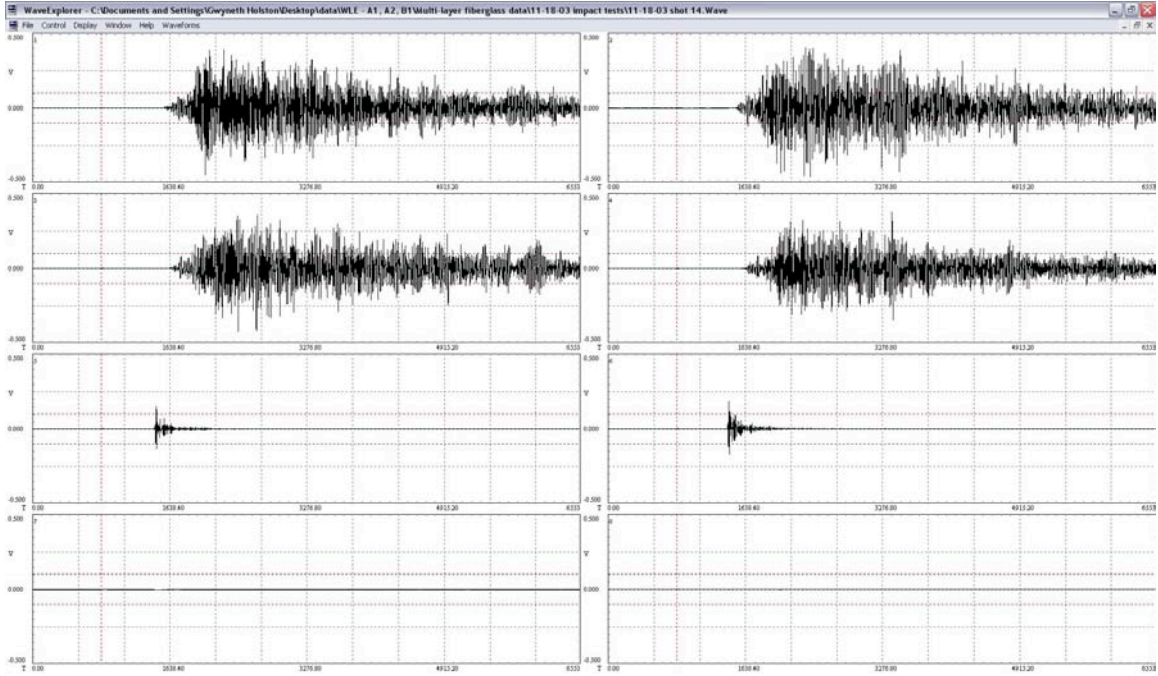


Figure 59: A-2 Shot #14 Impact Waveform

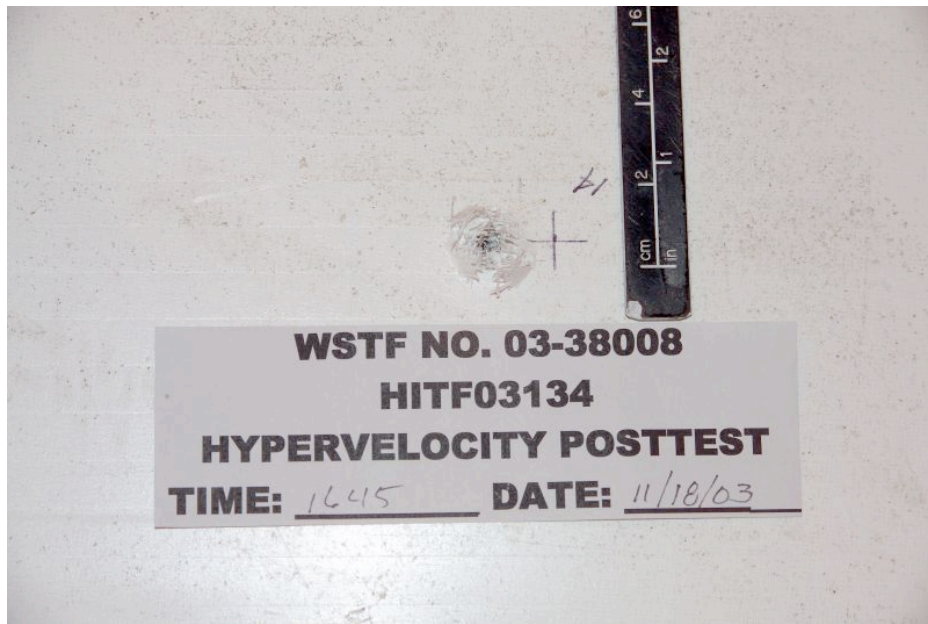


Figure 60: A-2 Shot #14 Impact Damage

Test conditions for AE (ultrasonic) data acquisition during hypervelocity impact testing

Test date: 11-14-03

Specimen description: 30X30X1 in. Fiberglass target with Aluminum 2nd layer
Target A-1
Shot # 15

Impact conditions:

Projectile material and diameter: 0.4 mm diameter aluminum
Planned impact coordinates (in.): 20, 20
Actual impact coordinates (in.): 20.4, 20.4
AE estimated impact coordinates (in.):
Planned impact velocity (km/s): 6.8
Actual impact velocity (km/s): 6.67
Impact angle: 0

Sensor information:

Ch. #	Sensor Model	x coord. (in.)	Y coord. (in.)	Attenuation at sensor * (dB)	Preamp gain/attenuation (dB)	System gain (dB)	Total gain/attenuation (dB)
1	225	8	5 (Al)	0	0	30	30
2	225	22	5 (Al)	0	0	30	30
3	225	8	25 (Al)	0	0	30	30
4	225	22	25 (Al)	0	0	30	30
5	225	6	7 (FG)	-50	0	33	-17
6	225	25	15 (FG)	-50	0	33	-17

20 Preliminary estimate for attenuation at sensor based on field measurements. Attenuators calibrated for 50 ohm input, but used for high impedance preamp input. Further laboratory characterization required.

Signal filter settings: 20kHz – 1500 kHz bandpass on all channels

Instrumentation settings:

5 MHz sampling rate
32k points
4096 pretrigger points

Comments: All signals in range except. Very small signal on Channel 5 that is suspect because of problem later found to be bad input connector on preamp.

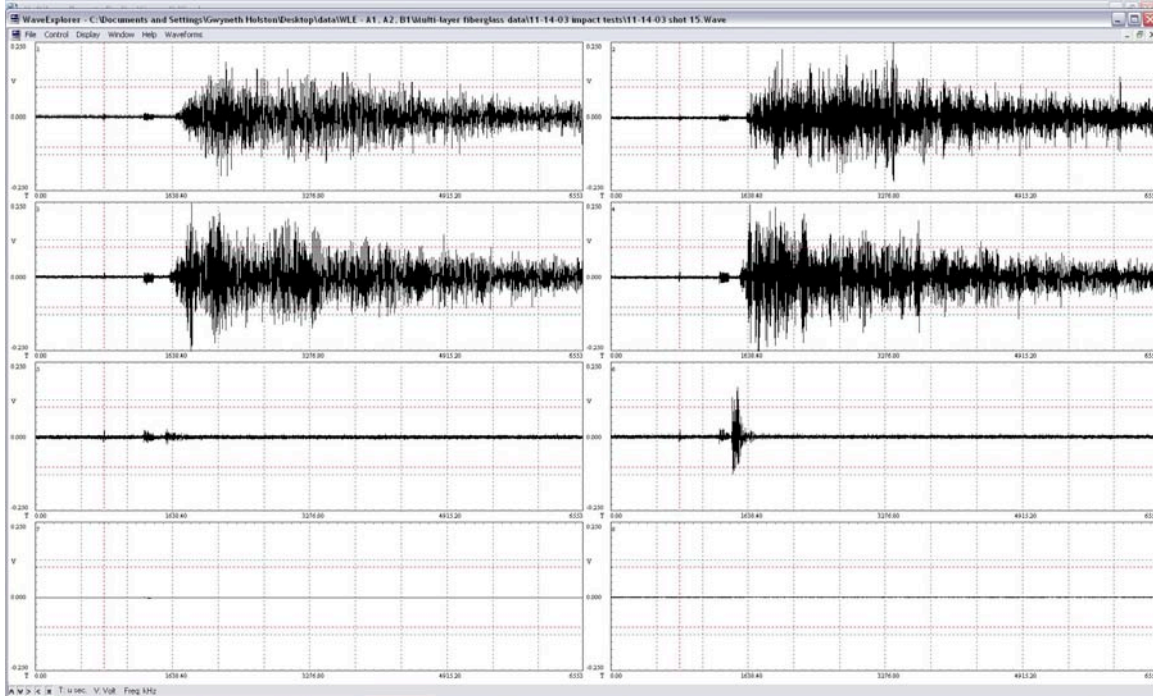


Figure 61: A-2 Shot #15 Impact Waveform



Figure 62: A-2 Shot #15 Impact Damage

Test conditions for AE (ultrasonic) data acquisition during hypervelocity impact testing

Test date: 11-18-03

Specimen description: 30X30X1 in. Fiberglass target with Aluminum 2nd layer
 No grommets around standoff rods
 Target A-2
 Shot # 16

Impact conditions:

Projectile material and diameter: 0.4 mm diameter aluminum
 Planned impact coordinates (in.): 12, 15
 Actual impact coordinates (in.): missed target
 AE estimated impact coordinates (in.):
 Planned impact velocity (km/s): 6.8
 Actual impact velocity (km/s): missed target
 Impact angle: 0

Sensor information:

Ch. #	Sensor Model	x coord. (in.)	Y coord. (in.)	Attenuation at sensor * (dB)	Preamp gain/attenuation (dB)	System gain (dB)	Total gain/attenuation (dB)
1	225	8	5 (Al)	0	0	15	15
2	225	22	5 (Al)	0	0	15	15
3	225	8	25 (AL)	0	0	15	15
4	225	22	25 (AL)	0	0	15	15
5	225	6	7 (FG)	-50	0	27	-23
6	225	25	15 (FG)	-50	0	27	-23

20 Preliminary estimate for attenuation at sensor based on field measurements. Attenuators calibrated for 50 ohm input, but used for high impedance preamp input. Further laboratory characterization required.

Signal filter settings: 20kHz – 1500 kHz bandpass on all channels

Instrumentation settings:

5 MHz sampling rate
 32k points
 4096 pretrigger points

Comments: System triggered, but no signals detected. Projectile missed target.

Data Tables

Test	Imp Dia	Imp Vel	Imp Ang	K.E.	Location	
No.	mm	km/s	deg	J	x	y
A1-1	1.0	6.71	90	31.83	12.6	20.7
A1-2	1.4	6.72	90	87.59	16.1	20.1
A1-3	1.6	6.67	90	128.81	20.2	9.75
A1-5	5.6	6.86	90	5841.76	20.2	17.1
A1-6	6.0	6.82	90	7101.57	11.9	9.75
B1-7	1.6	6.82	90	134.67	11.8	19.6
B1-8	2.0	6.75	90	257.65	11.9	9.6
B1-9	5.6	6.96	90	6013.32	18	19.2
B1-10	6.0	6.85	90	7164.18	17.8	10.1
A2-11	1.0	6.72	90	31.92	11.8	19.7
A2-12	1.4	6.62	90	85.00	17.5	19.9
A2-13	1.6	6.69	90	129.58	12.3	10.1
A2-14	2.0	6.75	90	257.65	18.6	10.1
A2-15	0.4	6.67	90	2.01	20.4	20.4

Table 3: A-1, B-1, and A-2 Impactor Diameter, Impactor Velocity, Impactor Angle, Kinetic Energy, and Location

Shot #4 had no recorded kinetic energy.

Test	Kinetic Energy	Crater Dims			Crater Vol	Damage Dims		Damage Area
		x	y	z		x	y	
No.	J	mm	mm	mm	mm ³	mm	mm	mm ²
A1-1	31.83	7.0	9.0	2.0	126.0	8.0	10.0	80.0
A1-2	87.59	9.0	10.0	2.5	225.0	13.5	17.0	229.5
A1-3	128.81	11.0	13.0	4.5	643.5	13.0	16.0	208.0
A1-4		13.0	13.0	7.4	1244.9	19.0	27.0	513.0
A1-5	5841.76	18.0	18.0	7.4	2386.6	19.0	27.0	513.0
A1-6	7101.57	23.0	25.0	7.4	4235.5	290.0	310.0	89900.0
B1-7	134.67	6.0	6.0	5.0	180.0	17.0	17.0	289.0
B1-8	257.65	7.0	7.0	1.5	73.5	23.0	17.0	391.0
B1-9	6013.32	21.0	19.5	7.4	3016.4	67.0	50.0	3350.0
B1-10	7164.18	25.5	24.0	7.4	4508.0	57.0	34.0	1938.0
A2-11	31.92	3.5	3.0	2.0	21.0	9.0	7.0	63.0
A2-12	85.00	5.0	6.0	4.0	120.0	16.0	13.0	208.0
A2-13	129.58	6.0	7.0	6.0	252.0	12.5	9.5	118.8
A2-14	257.65	5.0	5.0	7.4	184.2	18.0	22.0	396.0
A2-15	2.01	1.0	1.0	0.2	0.2	1.5	1.5	2.3

Table 4: A-1, B-1, and A-2 Damage Results

Shot #4 had no recorded kinetic energy.

Test	S1 RawEn	S2 RawEn	S3 RawEn	S4 RawEn	S5 RawEn	S6 RawEn	S7 RawEn	S8 RawEn
No.	V ² -μs	V ² -μs	V ² -μs	V ² -μs	V ² -μs	V ² -μs	V ² -μs	V ² -μs
A1-1	8.365E-01	1.087E+00	9.590E-01	5.674E-01	1.691E-04	2.177E-04		
A1-2	2.332E+01	2.724E+01	3.472E+01	1.728E+01	2.911E-01	7.092E-01		
A1-3	8.351E-06	9.710E-06	1.357E-05	1.551E-05	7.943E-06	1.121E-05		
A1-5	1.014E+03	3.083E+02	9.966E+02	3.535E+02	8.077E+00	1.078E+01		
A1-6	5.267E+00	1.680E+01	1.904E+01	8.932E+00	4.160E-02	6.058E-02		
B1-7	2.122E+00	2.684E+00	1.389E+01	4.089E+00	2.998E-01	9.612E-01	7.402E+00	1.051E+01
B1-8	1.095E+02	8.668E+00	1.015E+01	3.245E+00	1.271E-03	3.345E-02	1.342E+00	1.440E+00
B1-9	2.975E-01	1.517E+00	1.763E+00	1.780E+01	1.004E-01	8.805E-01	6.602E-02	6.888E-02
B1-10	1.124E-01	7.745E-01	5.525E-02	1.385E-01	1.317E-01	1.868E-01	8.948E+01	8.293E+01
A2-11	6.272E+02	6.875E+02	7.033E+02	4.555E+02	1.070E-01	2.004E-01		
A2-12	1.348E+01	3.327E+01	1.950E+01	1.140E+01	1.622E-03	8.177E-01		
A2-13	5.493E+00	8.821E+00	8.778E+00	4.146E+00	4.699E-01	1.704E-01		
A2-14	3.930E+01	5.142E+01	3.699E+01	2.792E+01	2.782E-01	5.554E-01		
A2-15	8.898E+00	1.129E+01	1.286E+01	1.261E+01	5.620E-02	4.512E-01		

Table 5: A-1, B-1, and A-2 Raw Wave Signal, Sensors 1-8
Shot #4 had no recorded kinetic energy.

Test	Channel Gain							
	1	2	3	4	5	6	7	8
A1-1	-20	-20	-20	-20	-50	-50		
A1-2	6	6	6	6	-41	-41		
A1-3	0	0	0	0	-50	-50		
A1-5	36	36	36	36	-37	-37		
A1-6	12	12	12	12	-58	-58		
B1-7	6	6	6	6	-64	-64	3	3
B1-8	-8	-8	-8	-8	-58	-58	-8	-8
B1-9	-38	-38	-38	-38	-52	-52	-18	-18
B1-10	-52	-52	-52	-52	-58	-58	3	3
A2-11	12	12	12	12	-38	-38		
A2-12	9	9	9	9	-41	-41		
A2-13	-17	-17	-17	-17	-47	-47		

A2-14	-17	-17	-17	-17	-47	-47		
A2-15	30	30	30	30	-17	-17		

Table 6: A-1, B-1, and A-2 Channel Gain Settings

Shot #4 had no recorded kinetic energy.

Test No.	S1 En J x 10 ⁻¹⁰	S2 En J x 10 ⁻¹⁰	S3 En J x 10 ⁻¹⁰	S4 En J x 10 ⁻¹⁰	S5 En J x 10 ⁻¹⁰	S6 En J x 10 ⁻¹⁰	S7 En J x 10 ⁻¹⁰	S8 En J x 10 ⁻¹⁰	TOT W.S.E. nJ
A1-1	8.365E+01	1.087E+02	9.590E+01	5.674E+01	1.691E+01	2.177E+01			3.836E+01
A1-2	5.859E+00	6.842E+00	8.722E+00	4.342E+00	3.664E+03	8.928E+03			1.262E+03
A1-3	8.351E-06	9.710E-06	1.357E-05	1.551E-05	7.943E-01	1.121E+00			1.915E-01
A1-5	2.546E-01	7.745E-02	2.503E-01	8.880E-02	4.048E+04	5.405E+04			9.453E+03
A1-6	3.323E-01	1.060E+00	1.201E+00	5.635E-01	2.625E+04	3.822E+04			6.447E+03
B1-7	5.329E-01	6.741E-01	3.490E+00	1.027E+00	7.530E+05	2.415E+06	3.710E+00	5.265E+00	3.168E+05
B1-8	6.907E+02	5.469E+01	6.404E+01	2.047E+01	8.022E+02	2.111E+04	8.465E+00	9.083E+00	2.276E+03
B1-9	1.877E+03	9.572E+03	1.113E+04	1.123E+05	1.591E+04	1.396E+05	4.166E+00	4.346E+00	2.904E+04
B1-10	1.781E+04	1.227E+05	8.757E+03	2.195E+04	8.308E+04	1.179E+05	4.485E+01	4.156E+01	3.723E+04
A2-11	3.958E+01	4.338E+01	4.438E+01	2.874E+01	6.750E+02	1.265E+03			2.096E+02
A2-12	1.698E+00	4.189E+00	2.455E+00	1.435E+00	2.042E+01	1.029E+04			1.032E+03
A2-13	2.753E+02	4.421E+02	4.400E+02	2.078E+02	2.355E+04	8.539E+03			3.345E+03
A2-14	1.970E+03	2.577E+03	1.854E+03	1.399E+03	1.394E+04	2.784E+04			4.958E+03
A2-15	8.898E-03	1.129E-02	1.286E-02	1.261E-02	2.817E+00	2.261E+01			2.548E+00

Table 7: A-1, B-1, and A-2 Wave Signal Energy, Sensors 1-8 and Total Wave Signal Energy

Shot #4 had no recorded kinetic energy.

REPORT DOCUMENTATION PAGE

*Form Approved
OMB No. 0704-0188*

The public reporting burden for this collection of information is estimated to average 1 hour per response, including the time for reviewing instructions, searching existing data sources, gathering and maintaining the data needed, and completing and reviewing the collection of information. Send comments regarding this burden estimate or any other aspect of this collection of information, including suggestions for reducing this burden, to Department of Defense, Washington Headquarters Services, Directorate for Information Operations and Reports (0704-0188), 1215 Jefferson Davis Highway, Suite 1204, Arlington, VA 22202-4302. Respondents should be aware that notwithstanding any other provision of law, no person shall be subject to any penalty for failing to comply with a collection of information if it does not display a currently valid OMB control number.
PLEASE DO NOT RETURN YOUR FORM TO THE ABOVE ADDRESS.

1. REPORT DATE (DD-MM-YYYY) 01-09 - 2007			2. REPORT TYPE Contractor Report		3. DATES COVERED (From - To)	
4. TITLE AND SUBTITLE Hypervelocity Impact (HVI) - Volume 2: WLE Small-Scale Fiberglass Panel Flat Multi-Layer Targets A-1, A-2, and B-1					5a. CONTRACT NUMBER NNL05AC19T	
					5b. GRANT NUMBER	
					5c. PROGRAM ELEMENT NUMBER	
6. AUTHOR(S) Gorman, Michael R.; and Ziola, Steven M.					5d. PROJECT NUMBER	
					5e. TASK NUMBER	
					5f. WORK UNIT NUMBER 377816.06.03.03.06	
7. PERFORMING ORGANIZATION NAME(S) AND ADDRESS(ES) NASA Langley Research Center Hampton, VA 23681-2199					8. PERFORMING ORGANIZATION REPORT NUMBER	
9. SPONSORING/MONITORING AGENCY NAME(S) AND ADDRESS(ES) National Aeronautics and Space Administration Washington, DC 20546-0001					10. SPONSOR/MONITOR'S ACRONYM(S) NASA	
					11. SPONSOR/MONITOR'S REPORT NUMBER(S) NASA/CR-2007-214885/Vol2	
12. DISTRIBUTION/AVAILABILITY STATEMENT Unclassified - Unlimited Subject Category 70 Availability: NASA CASI (301) 621-0390						
13. SUPPLEMENTARY NOTES Langley Technical Monitor: Eric I. Madaras An electronic version can be found at http://ntrs.nasa.gov						
14. ABSTRACT During 2003 and 2004, the Johnson Space Center's White Sands Testing Facility in Las Cruces, New Mexico conducted hypervelocity impact tests on the space shuttle wing leading edge. Hypervelocity impact tests were conducted to determine if Micro-Meteoroid/Orbital Debris impacts could be reliably detected and located using simple passive ultrasonic methods. The objective of Targets A-1, A-2, and B-2 was to study hypervelocity impacts through multi-layered panels simulating Whipple shields on spacecraft. Impact damage was detected using lightweight, low power instrumentation capable of being used in flight.						
15. SUBJECT TERMS Hypervelocity impact tests; Space shuttle; Wing leading edge; Debris; Impact damage						
16. SECURITY CLASSIFICATION OF:			17. LIMITATION OF ABSTRACT	18. NUMBER OF PAGES	19a. NAME OF RESPONSIBLE PERSON	
a. REPORT	b. ABSTRACT	c. THIS PAGE			STI Help Desk (email: help@sti.nasa.gov)	
U	U	U	UU	69	19b. TELEPHONE NUMBER (Include area code) (301) 621-0390	